

DYNAMIC NEURAL CORRELATES OF MENTAL ATTENTION CAPACITY

AMIR ZARIE

A THESIS SUBMITTED TO

THE FACULTY OF GRADUATE STUDIES

IN PARTIAL FULFILMENT OF THE REQUIREMENTS FOR THE DEGREE OF

MASTER OF ARTS

GRADUATE PROGRAM IN PSYCHOLOGY

YORK UNIVERSITY

TORONTO, ONTARIO

OCTOBER 2020

© Amir Zarie, 2020

## **Abstract**

Mental attention capacity (M-capacity) – the maximum amount of information one can process simultaneously – is a predictor of academic and professional success. However, its neural underpinnings are not well understood. Here, a novel implementation of dynamic functional connectivity (dFC) analysis of resting-state functional MRI data – with parcellation of individual brains into a common set of functional areas (Group Prior Individual Parcellation, GPIIP) – was used to determine whether dFC is 1) related to individual differences in M-capacity and 2) modulated by prior performance of a demanding M-capacity task. Additionally, the novel dFC approach using GPIIP was validated against a well-established dFC method (Group ICA of fMRI Toolbox, GIFT). While one measure of dFC accounted for individual differences in M-capacity, dFC was not modulated by prior task performance. The novel dFC analysis using GPIIP produced similar results to GIFT dFC, demonstrating the validity and potential advantages of this novel approach to dFC analysis.

## **Acknowledgements**

I would like to acknowledge my parents and my brothers who have always supported me in my decisions and for fostering my sense of curiosity. You have always been there for me during cheerful and challenging times.

I would like to thank Dr. Dale Stevens for his guidance throughout my master's degree and inspiring me to learn and to improve. I would also like to acknowledge all my lab mates for helping me and teaching me about neuroscience and research in this field. I would like to also thank Mylann Guevara for bringing me onboard her study so I can conduct my secondary analysis.

## Table of Contents

Abstract.....	ii
Acknowledgements.....	iii
Table of Contents.....	iv
List of Tables.....	vii
List of Figures.....	viii
List of Appendices.....	x
Introduction.....	1
Neuroscientific Approach.....	2
Objectives.....	5
Hypotheses.....	5
Methods.....	6
Participants.....	6
Materials & Apparatus.....	7
Behavioural Tasks.....	7
MRI Data Acquisition Parameters.....	7
Analysis.....	8
Behavioural Analysis.....	8

Preprocessing.....	8
Dynamic Functional Connectivity Analysis.....	12
Demographic Data for Final Analyses.....	13
Conducting Dynamic Functional Connectivity Analysis Using GIFT.....	14
Results.....	14
Results Related to Testing of the First Hypothesis.....	14
Neural Flexibility and M-Capacity.....	14
Clown Task Results and M-Capacity Scores.....	15
Dynamic Functional Connectivity Results: All Pre-Resting-State fMRI.....	16
State Change Results: Pre-Resting-State fMRI.....	19
Dwell Time Results: Pre-Resting-State fMRI.....	23
Comparison of States Between the High and Low M-Capacity Groups.....	29
Results Related to Testing of the Second Hypothesis.....	31
State Change and Dwell Time Between the Pre- and Post-Resting-State fMRI...31	
Comparison of Pre- and Post-States.....	33
Results Related to Testing of the Third Hypothesis.....	35
Supplemental Analyses.....	36
Correlation of M-Capacity With State Change and Dwell Time of Post-Resting- State fMRI.....	36

Discussion.....	40
Neural Flexibility and M-Capacity.....	40
Modulation of Dynamic Functional Connectivity.....	41
Use of GPIP to Conduct Dynamic Functional Connectivity Analysis.....	42
Supplemental Analysis of M-Capacity and Dynamic Functional Connectivity.....	42
Comparison of Results With Prior Studies Using DFC Analysis.....	43
Future Directions.....	45
Limitations.....	45
Conclusion.....	46
References.....	47
Appendices.....	51

## List of Tables

Table 1: Demographic Information of Participants in Each Analysis.....	14
--	----

## List of Figures

Figure 1: Sample Preprocessed Images for Quality Control.....	10
Figure 2: Sample Parcellation With GPIP.....	11
Figure 3: Quality Control of Participant’s GPIP Based on Functional Connectivity.....	11
Figure 4: Average M-Capacity Scores for the High and Low Groups.....	16
Figure 5: Pre-State 1.....	17
Figure 6: Pre-State 2.....	18
Figure 7: Standard Deviation of Pre-State 1 and 2.....	19
Figure 8: Average of Pre-State Change for High and Low M-Capacity Groups.....	20
Figure 9: Ranked Correlation Between M-Capacity and Pre-State Change.....	21
Figure 10: Average Pre-State Change for High and Low M-Capacity Groups (Separate Analysis).....	22
Figure 11: Ranked Correlation Between Low M-Capacity Group’s Scores and Pre-State Change.....	23
Figure 12: Average Dwell Time of in States 1 and 2 for High and Low M-capacity Groups.....	24
Figure 13: Ranked Correlation Between M-Capacity Scores and Average Dwell Time in State 1.....	25
Figure 14: Ranked Correlation Between M-Capacity Scores and Average Dwell Time in State 2.....	26



Figure 15: Average Dwell Time of High and Low M-capacity Groups in Pre-States 1 and 2...	27
Figure 16: Ranked Correlation Between Low Group's M-Capacity Scores and Average Dwell Time in State 1.....	28
Figure 17: Ranked Correlation Between Low Group's M-Capacity Scores and Average Dwell Time in State 2.....	29
Figure 18: Correlation Difference and P-Values of State 1 Between High and Low M-Capacity Groups.....	30
Figure 19: Correlation Difference and P-Values of State 2 Between High and Low M-Capacity Groups.....	31
Figure 20: Average State Change of Pre- and Post-Task rsfMRI Sessions.....	32
Figure 21: Average Dwell Time of High and Low M-Capacity Groups in Pre- and Post-States 1 and 2.....	33
Figure 22: Correlation Difference and P-Values Between Pre- and Post-State 1.....	34
Figure 23: Correlation Difference and P-Values Between Pre- and Post-State 2.....	35
Figure 24: States Obtained From Dynamic Functional Connectivity Analysis Using GIFT.....	36
Figure 25: Ranked Correlation Between M-Capacity Scores and Post-State Change.....	37
Figure 26: Ranked Correlation Between M-Capacity Scores and Dwell Time in Post-State 1...38	
Figure 27: Ranked Correlation Between M-Capacity Scores and Dwell Time in Post-State 2...39	

## **List of Appendices**

Appendix A: Sample Clown version of Colour Matching Task.....	51
Appendix B: States From Conducting Dynamic Functional Connectivity on High and Low M- Capacity Groups Separately.....	52
Appendix C: Post-Resting-State fMRI States.....	53
Appendix D: Sample Dynamic Functional Connectivity Results From Literature.....	54

## Introduction

The ability to reason and use information in a goal-directed manner is a central topic in cognitive neuroscience and has been shown to be a strong predictor of academic and professional success, socioeconomic status, and even longevity (Deary, 2012). Various theories have been proposed to explain and quantify cognitive abilities related to information processing. Most relevantly, Pascual-Leone (1970) proposed the theory of Constructive Operators (TCO).

The TCO predicts a stepwise increase across development in an individual's capacity to process information, corresponding to the Piagetian stages of development (Chapman, 1981; Kemps et al., 2000). As such, it explains patterns of cognitive growth through development (Pascual-Leone, 1970; Pascual-Leone and Johnson, 2005). Broadly, the TCO is composed of schemes and operators. Schemes are information-bearing contents that inform experience and can shape behaviour (Pascual-Leone and Johnson, 2005). Alternatively, operators are non-informational and serve the function of selecting and synthesizing schemes. Importantly, M-capacity is an operator that activates task-relevant schemes, and the I-operator suppresses task-irrelevant schemes.

The TCO posits that there is a limit to the amount of information one can store and process at any given time. Specifically, the information load of a task, described as the number of active schemes required for successful completion of the task, is referred to as M-demand. The individual must possess equal or higher M-capacity than the M-demand to be able to overcome the challenges posed by the task (Chapman, 1981). Empirically, it has been shown that M-capacity is best measured when the I-operator is simultaneously engaged by requiring the individual to suppress irrelevant information. The presence of misleading cues limits the number of "slots" available in M-capacity to allocate to other cognitive resources (Pascual-Leone, 2000).

Tasks such as Color Matching Tasks (CMT) were designed for such valid assessment of M-capacity and have been shown to accurately assess of M-capacity (Arsalidou et al., 2010). Appendix A provides sample stimuli for the Clown version of the CMT, which will be considered in this study. So far, the underlying neural processes of M-capacity have not been extensively studied and remain poorly understood. Recently developed analyses that quantify behaviourally relevant dynamics in brain activity can be used to investigate the neural systems underlying M-capacity. This will provide information about the neural underpinnings of the TCO more broadly.

### **Neuroscientific approach**

Neuroimaging techniques used in research have contributed immensely to the neural basis of theories of cognitive processing. Functional magnetic resonance imaging (fMRI) is used for non-invasive imaging of brain activity. It provides an indirect measure of brain activity by detecting localized changes in relative blood oxygenation, referred to as blood-oxygen-level-dependent (BOLD) signal (Hillman, 2014). Many studies have investigated how brain activity, measured by BOLD signal time series, relates to cognitive processing. Specifically, functional connectivity (FC) analysis, which provides a measure of statistical dependence of BOLD signal across time between various regions of interest (ROI)s in the brain, is related to behavioural measures (Stevens & Spreng, 2014). A popular method for obtaining a measure of FC is to correlate the entire mean time series of the ROIs. However, this approach yields a “static” measure of FC referred to as sFC, since it assumes that the variation in FC is stationary (Hutchison et al., 2013). It has also been shown that the time series is not, in fact, stationary (Hutchison et al., 2013). Therefore, novel methods have been used to quantify the temporal dynamics of FC referred to as dynamic FC (dFC) (Hutchison et al., 2013).

It has been shown that dissociable patterns of resting-state FC (RSFC) revealed through sFC analysis are related to individual differences in cognition, emotion, and long-lasting behavioural patterns (e.g., personality traits) (Adelstein et al., 2011; Stevens and Spreng, 2014). Furthermore, using RSFC data, Jia et al. (2014) demonstrated that compared to sFC, dFC analysis accounted for a higher proportion of variability across 75 different behavioural domains such as alertness, cognition, emotion, and personality traits. This shows that the temporal features of the BOLD signal time series should be accounted for, since they contain behaviourally relevant information. However, the neural underpinnings of M-capacity have not been explored with dFC. Therefore, there is a gap in our understanding of how the temporal features of FC are related to M-capacity. The proposed research will investigate this question.

Resting-state functional connectivity strength is greater in adults compared to children among brain areas underlying language processing, such as Wernicke's and Broca's areas (Koyama et al., 2011). This indicates that RSFC adapts through development in accordance with the acquired skill. Furthermore, it was found that RSFC changes in even shorter times scales as a result of a visual search training task (Bueichekú et al., 2019; Lewis, Baldassarre, et al., PNAS, 2009). These findings indicate that RSFC is modulated by the task the individual was previously engaged in. Waites et al. (2005) found that functional connectivity between left and right middle frontal gyri, and between posterior cingulate and medial frontal cortex were strengthened in the resting-state following a language task. Their findings provide evidence that RSFC reflects the moment-to-moment changes in cognitive states. Another study by Stevens et al. (2010) showed that viewing category specific visual stimuli modulated the coupling of the respective category preferential regions during subsequent rest. The extant literature substantiates that the present cognitive state and fluctuations in brain activity are modulated by prior cognitive states and

fluctuations in brain activity in a meaningful way. However, it is unclear how the temporal features of RSFC are modulated by prior engagement in a cognitively demanding task, such as tasks that measure M-capacity. This will also be investigated in this study.

To perform dFC analysis, a fixed size sliding window correlation is applied to the BOLD time series derived from the parcellated cortex. The parcellated cortex is a map delineating the boundaries between different brain regions. Then, k-means clustering is applied to the FC matrices to group similar matrices into the same cluster referred to as a state. Each brain state signifies a stable FC configuration through which the brain transitions. Since previous work showed that neural flexibility during rest is related to cognitive processing (Nomi et al., 2017), it is expected that dFC measures indicating greater flexibility would account for individual differences on M-capacity scores. Furthermore, it would also be expected that dFC measures of RSFC would differ between the resting-state data collected before and after the behavioral task - measuring the participant's M-capacity – based on literature indicating that RSFC is modulated by the prior task.

Commonly, an open source analysis tool called GIFT is used to conduct dFC analysis (<http://mialab.mrn.org/software/gift/>). There are three main differences between the GIFT method of conducting dFC and the approach used in the current study: 1) the parcellation of brain images: the current study uses a program called Group Prior Individual Parcellation (GPIP) (Chong et al., 2017), which parcellates the brain based on RSFC. However, GIFT uses independent component analysis (ICA) to parcellate the brain based on maximal statistical independence. As such, the components (parcels) do not necessarily correspond to functionally meaningful regions and they may outline a mixture of different brain regions.; 2) taking into consideration individual differences in the same brain regions: GIFT uses group averaged

measures to parcellate the brain. This means that it does not take into consideration the differences in the location of the same brain regions between individuals. However, GPIIP uses individualized brain parcellation to extract the timer series; 3) inclusion of several types of brain tissues (e.g. grey and white matter) as opposed to just grey matter: GIFT uses data from the different types of brain tissue. This may introduce additional noise in the data. However, GPIIP only uses data obtained from the surface of the cortex. Even though the primary goal of the current study is not to rigorously compare the two methods, no study has used GPIIP to conduct dFC analysis. Therefore, this study also serves as a proof of concept for how GPIIP can be used in the dFC analysis stream. To do so, a summary of the dFC results from both analysis streams will be provided for qualitative comparison. Despite the differences between the two methods, the overall properties of dFC is expected to be similar.

## **Objectives**

The objective of the current proposal is to investigate the neural basis of M-capacity. DFC analysis will be applied to take into consideration the temporal dynamics of FC. Specifically, the study aims to (1) characterize how dFC measures of RSFC account for individual differences in scores on M-capacity tasks and (2) characterize how dFC is modulated by engaging in cognitively demanding tasks relying on M-capacity, and (3) provide preliminary evidence that it is feasible to conduct dFC with data obtained from GPIIP and show that the results will be similar to dFC conducted with GIFT.

## **Hypotheses**

Based on previous literature showing that neural flexibility is related to cognitive performance (Jia et al., 2014), it is hypothesized that measures of dFC applied to resting-state

data related to flexibility in neural processing will significantly account for individual differences on scores of M-capacity. There are several different measures of flexibility, such as higher number of state changes and higher dwell time in a state characterized by higher variability. Whereas the former defines neural flexibility as the frequency with which the brain switches between stable states, the latter defines neural flexibility as the brain's ability to show more varied FC. Furthermore, it is expected that measures of dFC in resting-state data collected following performance of an M-capacity task (post-task rsfMRI) will display altered measures of dFC compared to resting-state fMRI data collected before the task (pre-task rsfMRI), due to the modulatory effects of the cognitively demanding task measuring M-capacity.

In addition, when comparing the analyses using GIFT to dFC using data parcellated with GPIP, it is predicted that the same number of states will be found, and these states will have similar FC structure and similar dFC metrics (i.e., state change and frequency of occurrence).

## **Methods**

### **Participants**

Previously collected resting-state fMRI and behavioural data from thirty healthy participants (16 females and 14 males) ranging between 20-30 years of age (Mean = 23, *SD* = 2.85) were used in the study. Participants were excluded based on the following conditions: neurological disorder, brain injury, left-handedness, abnormal vision that could not be corrected, non-proficiency with the English language, color blindness, or incompatibility with the MRI environment.



## **Materials & Apparatus**

### ***Behavioural Tasks***

The CMT is adapted from a 1-back task - introduced by Kirchner (1958) - to incrementally increase the demand on M-capacity (Arsalidou et al., 2010; Arsalidou et al., 2013). Further, the tasks were designed for use with children and adults. Both tasks require participants to attend to the stimuli and indicate whether the current stimulus shares the same set of features of interest with the previously viewed stimulus by pressing the appropriate button. Appendix A shows the Clown version of the CMT. Appendix A also portrays a sample task procedure used to collect the behavioural data. Briefly, in CMT, participants are instructed to ignore blue and green colors and pay attention to the following colors of interest: brown, grey, orange, pink, purple, red, and yellow. The stimulus is considered “same” if it contains the exact same colour-set, regardless of the location and number of the coloured items in the stimulus. The clown version of the CMT is made more difficult by asking the participants to ignore the face of the clown as well. There are six difficulty levels determined by the number of colors of interest that need to be attended to simultaneously, and the distracting colors in the clown’s face to be ignored.

### ***MRI Data Acquisition Parameters***

A 3T Siemens Magnetom Tim Trio scanner with a 32-channel head coil located at York MRI Facility was used to collect the brain imaging data. Anatomical images were acquired with a 3D magnetization prepared rapid gradient echo sequence (TR = 2300 ms; TE = 2.62 ms; 9° Flip angle; 1.0 mm isotropic voxels). Regarding the resting-state runs, 229 volumes were collected (TR = 2620 ms; TE = 14, 27, 40 ms; 83° Flip angle; 3.4 × 3.4 × 3.0 mm voxels; 43

interleaved slices covering the whole brain, including the cerebellum) for both the pre- and post-task rsfMRI sessions.

## **Analysis**

### **Behavioural Analysis**

The six levels of difficulty used to measure M-capacity correspond to the number of relevant elements the participant must attend to, which is denoted as  $n$ . Furthermore, to account for the executive demand and the number of irrelevant elements the participants must ignore, a value of 2 is added. Finally, M-capacity was computed using the highest level of difficulty of the Clown task that the participant passed with a minimum accuracy of 70% (Arsalidou et al., 2010; Arsalidou et al., 2013).

To conduct group analyses, the M-capacity scores were used to create Low and High M-capacity groups. Due to a ceiling effect in the M-capacity scores, the individuals who scored the highest (i.e., 6) were assigned to the High M-capacity group, and the remaining individuals were assigned to the Low M-capacity group.

### **Preprocessing**

Imaging data were preprocessed with AFNI (Cox, 1996). The raw data were de-spiked, shifted in time, aligned, and co-registered. Furthermore, tedana (DuPre et al., 2019) was used to optimally remove noise from the multi-echo data using ICA. The preprocessed data were then evaluated for their quality. The data from participants who showed excessive motion (higher than 1.5 mm) or had a high brain-wide average correlation were excluded from analyses. Figure 1 (left) shows an example of a participant's data that were discarded based on high brain-wide average correlation. Alternatively, participants' data such as the one displayed in Figure 1 (right)

were passed on to the next stage of processing. This resulted in discarding 3 participants' entire dataset out of the 30 participants. Then, FreeSurfer (Fischl, 2012) was used to extract the cortical surface images of each participant's anatomical data. GIP was used on the cortical surface and functional data to individually parcellate the entire cortex of each participant. Specifically, the atlas of Schaefer et al. (2018) was used to parcellate the brain into 100 different regions (50 nodes from each hemisphere combined) based on the 17-network model by Yeo et al. (2011). Then, the brain regions corresponding to the 17-network model were identified from the 100 regions and averaged to obtain the time series of the 17-network model. As such, 34 nodes were obtained in all, including the 17 nodes from each hemisphere. Figure 2 shows an example of a participant's functional data parcellated into 17 networks. To ensure high quality of the parcellation, correlation maps of all 100 regions were visually inspected. The data that did not display any network structure were discarded. Figure 3 (left) shows an example of correlation matrix that was discarded. However, correlation matrices resembling the matrix in Figure 3 (right) were retained for further processing. Specifically, if the correlation matrix demonstrated network structure and both high positive and negative correlation values were present, the data were included in the analysis. This step resulted in the elimination of 4 participants' entire dataset out of the 27 remaining participants.

## Sample Preprocessed Images for Quality Control

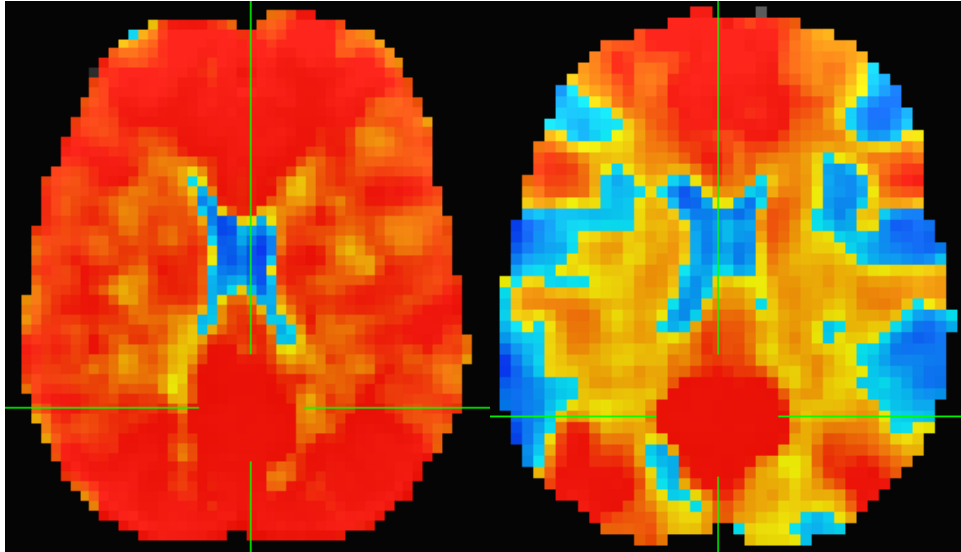


*Figure 1:* The left brain image shows an example of a participant's data that was discarded. The right brain image shows an example of a participant's data that was kept for further processing.

## Sample Parcellation With GPIP

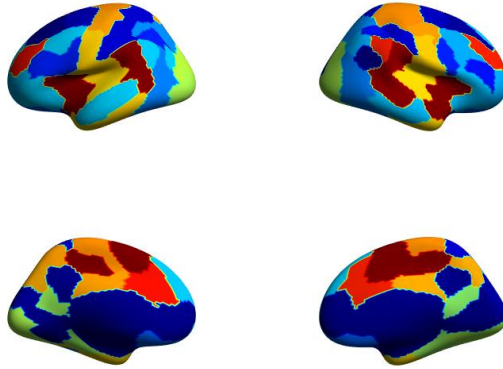


Figure 2: Example of a participant's functional data parcellated into 17 networks using the Schaefer et al. (2008) atlas with GPIP.

## Quality Control of Participant's GPIP Based on Functional Connectivity

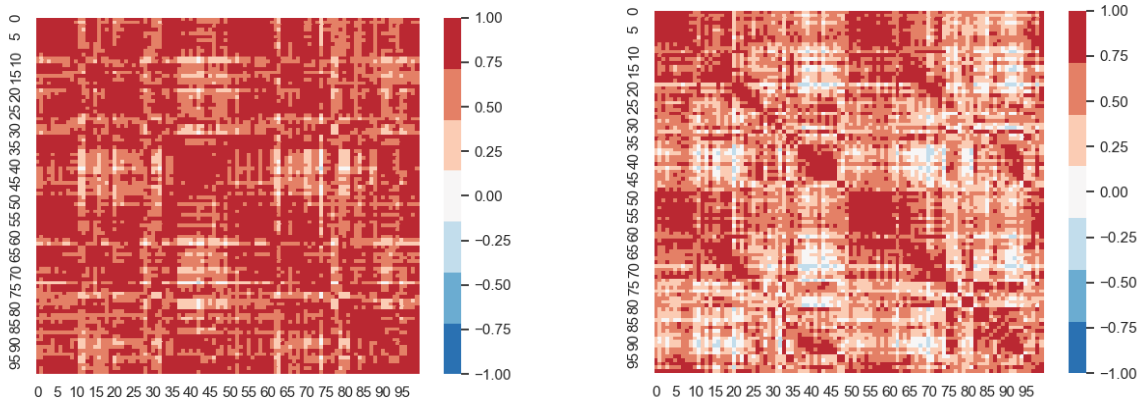


Figure 3: Shows correlation matrices for 2 participants. The color bar on the right indicates Pearson correlation values. The numbers on the x and y axes correspond to the 100 regions of the parcellated cortex. The left and right matrices are from poor and acceptable quality parcellated brain data, respectively. Only the data with acceptable parcellation were passed on for additional processing.

## Dynamic Functional Connectivity Analysis

DFC analysis was conducted on the time-series obtained from the parcellated images of the participants. To conduct dFC analysis, a sliding window of 23 TRs (approximately 60 seconds) was selected with a stride of 1 TR. Then, using a cross-validation method, the optimal L1 regularization value,  $\alpha$ , was computed using the inverse covariance matrix for each participant. This method ensures that important information in the graphical structure of the correlation matrices is not lost when the sliding window is applied to the data since there are more features than data points in the sliding window. This is done by creating a sparser inverse covariance matrix from which the correlation matrices are computed. The same penalization value was applied to regularize the covariance matrices computed over all sliding windows. Furthermore, the covariance matrices were converted to correlation measures and finally Fisher-z transformed. After applying this to each participant separately, data from the participants were concatenated. Then, a range of clusters was used to conduct K-means clustering and the optimal clustering value was selected based on the silhouette method. The silhouette method is a cluster validation strategy where the similarity of data points to their own cluster is compared to their similarity with other clusters. Higher average similarity of data points to their own cluster compared to other clusters indicates better clustering. The average of all correlation matrices within each cluster is referred to as a state which identifies the stable FC structure the brain occupies. Furthermore, measures such as state change and dwell time were computed and used to evaluate the hypotheses. State change was computed by first labelling the state of each correlation matrix from the sliding window and then counting the number of times there was a shift from one state to another. Dwell time was calculated by averaging the number of consecutive correlation matrices from the sliding windows that belong to a single state and the

unit is in TRs (i.e., whole fMRI volumes). Due to the algorithm not converging on a solution to compute the correlation matrices from the sliding windows, 4 participants' entire datasets were discarded. This resulted in the full analysis being conducted on 19 out of 30 participants. For the group analysis, 9 and 10 participants were assigned to the Low and High M-capacity groups, respectively. Finally, through the same preprocessing procedure outlined here and in the previous section, 8 participants' datasets were discarded out of the 16 participants who completed both the pre- and post-task rsfMRI sessions.

### **Demographic Data for Final Analyses**

Table 1 provides the demographic information of the participants that were included in the analyses to test each hypothesis. Specifically, 19 participants (9 females, 10 males) were included to test whether measures of dFC are related to M-capacity scores. Information regarding group differences in measures of dFC between High (6 females, 3 males) and Low (4 females, 6 males) M-capacity groups is also provided. To test whether measures of dFC are altered due to the intervening task, 8 participants' (1 females, 7 males) data out of the 16 participants who completed both the pre- and post-task rsfMRI sessions were included. Lastly, the same 19 participants data used to test the first hypothesis were included to compare dFC analysis with GPIP to GIFT.

## Demographic Information of Participants in Each Hypothesis

	Females		Mean Age for Females		Males		Mean Age for Males	
First Hypothesis: Combined	9		24.3		10		22.5	
First Hypothesis: Separate Groups	High: 6	Low: 3	High: 24.8	Low: 23.3	High: 4	Low: 6	High: 21.75	Low: 23
Second Hypothesis	1		23		7		23.6	
Third Hypothesis	9		24.3		10		22.5	

*Table 1:* Provides detailed demographics information such as number of females and males as well as their average age for the participants that were included to test each hypothesis.

## Conducting Dynamic Functional Connectivity Analysis Using GIFT

The preprocessed fMRI data were used to conduct dFC analysis with GIFT. To reiterate, the main difference is that GIFT uses ICA to parcellate the brain. As such, the data were parcellated into 50 components. Furthermore, all other parameters, such as length of sliding window, shifts in the sliding windows, and L1 regularization were kept the same.

## Results

### Results Related to Testing of the First Hypothesis

#### *Neural Flexibility and M-Capacity*

Based on previous literature, it was hypothesized that higher neural flexibility measured during rest would be related to higher M-capacity. This hypothesis was explicitly tested by comparing the average number of state changes and dwell time between two participant groups



during rest (before completing the task). Furthermore, the analysis was done in two different ways. In the first method, the state change and dwell time measures were extracted after running dFC on the pre-task rsfMRI for all participants combined. In the second method, dFC analysis was conducted on the High and Low M-capacity groups separately and then their average state change and dwell time were obtained for comparison. In contrast to the latter method, the former method assumes that the dFC is not significantly different between the two groups. In addition, correlations between M-capacity scores and the dFC measures were calculated to evaluate the strength of the relationship between these factors.

### ***Clown Task Results and M-Capacity Scores***

The scores on the Clown task were used as a measure of M-capacity to conduct the analyses. Due to lower overall variability and a ceiling effect in the behavioral data, the scores ( $n = 19$ ) here split into two groups by assigning participants who did not achieve a perfect score to the Low ( $M = 3.77$ ,  $SD = 1.61$ ,  $n = 9$ ) and the remaining participants who did achieve a perfect score to the High ( $M = 6$ ,  $SD = 0$ ,  $n = 10$ ) M-capacity group. Comparing the mean of M-capacity scores of the two groups, the Low group had significantly lower M-capacity than the High group ( $t(17) = -4.10$ ,  $p < 0.01$ ). Figure 4 shows a bar plot of M-capacity scores for High and Low groups. All error bars depicted in bar plots as well as shaded areas in correlation plots indicate standard deviation.

### Average M-Capacity Scores for the High and Low Groups

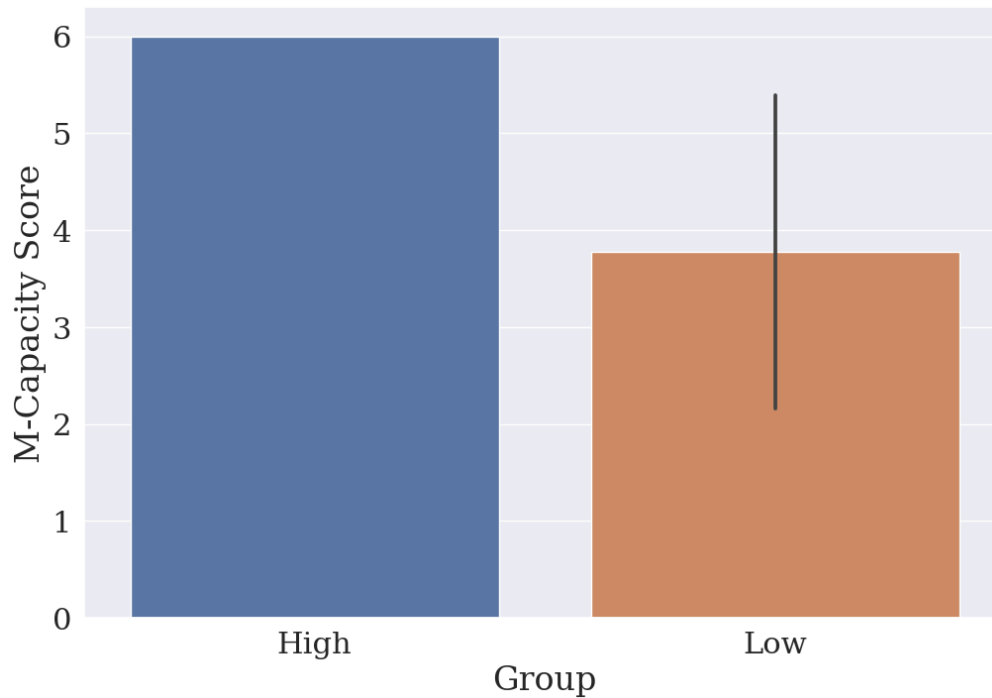


Figure 4: M-capacity scores of the High and Low groups. The High group ( $M = 6$ ,  $SD = 0$ ,  $n = 10$ ) had a significantly higher M-capacity score than the Low group ( $M = 3.77$ ,  $SD = 1.61$ ,  $n = 9$ ).

### ***Dynamic Functional Connectivity Results: All Pre-Resting-State fMRI***

The optimal number of states from the dFC analysis conducted on all pre-task rsfMRI data was found to be 2. Figures 5 and 6 display the states corresponding to states 1 and 2 referred to as pre-State 1 and pre-State 2. Pre-State 1 is characterized by zero or low positive correlation between all the regions. The participants spent most of the time in this state ( $M = 88.14\%$ ,  $SD = 13.65$ ). Pre-State 2 ( $M = 11.85\%$ ,  $SD = 13.65$ ) is characterized by moderate positive correlation between left hemisphere (LH) visual, somatomotor, dorsal attention, and salience/ventral attention networks and their corresponding regions in the right hemisphere (RH). In addition, the previously mentioned regions showed moderate anti-correlation with control and default mode network regions. The remaining regions showed zero or low positive correlation with the

remaining nodes. Figure 7 shows the standard deviation of pre-State 1 and 2 on the left and right, respectively; Pre-State 1 (with a mean standard deviation of 0.11) is characterized by higher average standard deviation than pre-State 2 (with a mean standard deviation of 0.01).

**Pre-State 1 ( $M = 88.14\%$ ,  $SD = 13.65$ )**

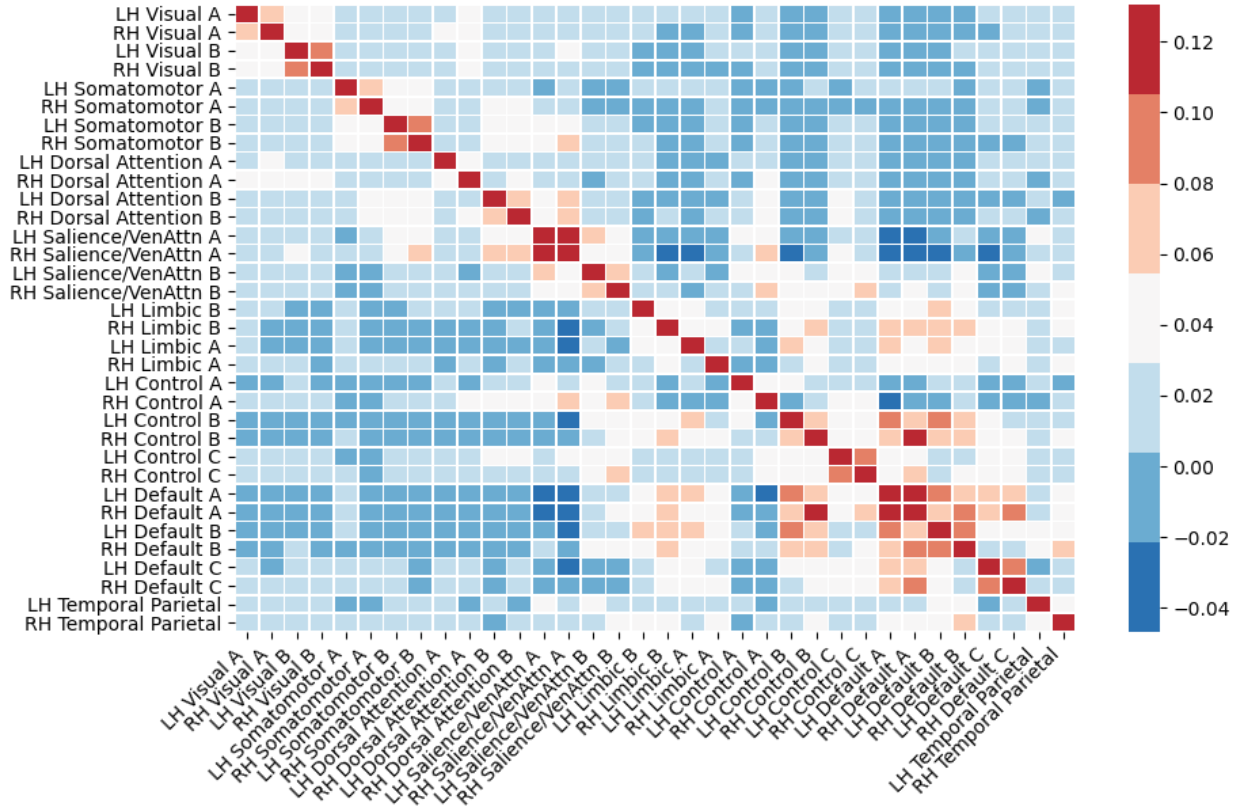
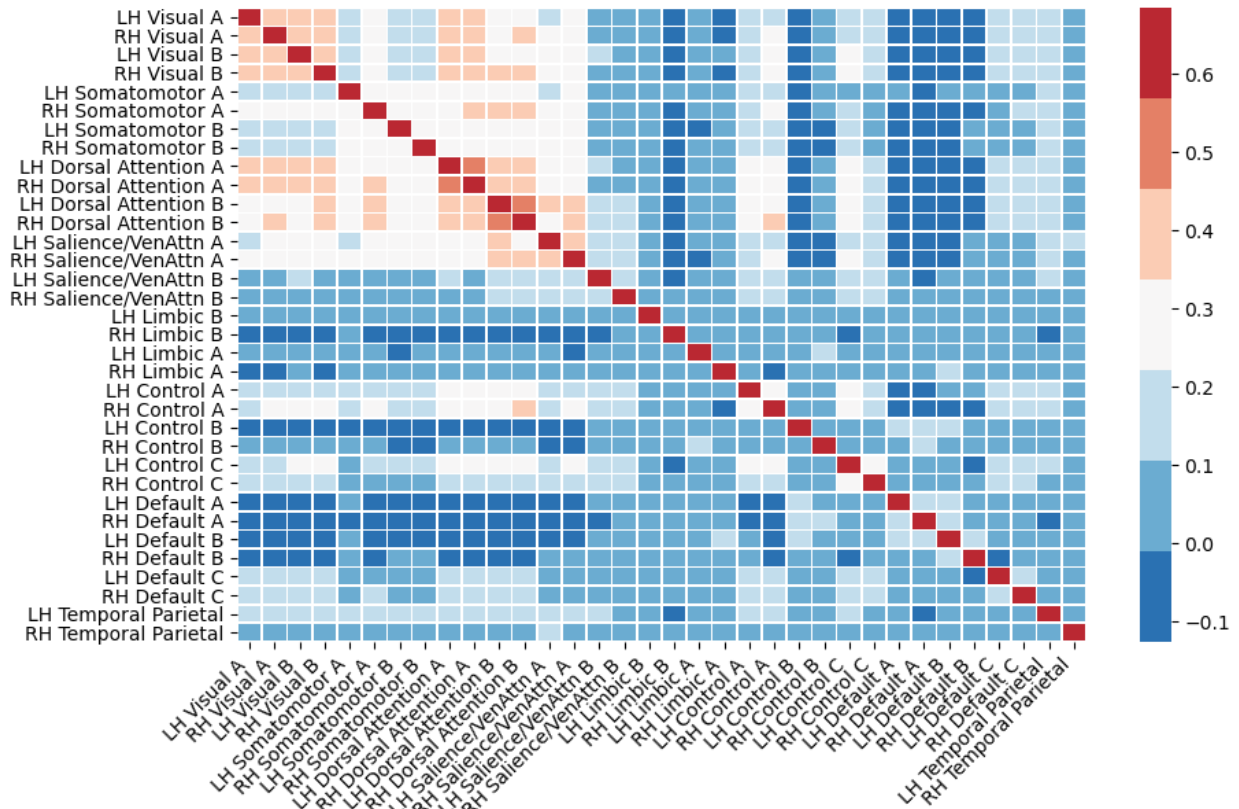


Figure 5: Pre-State 1. The color bar indicates the Pearson correlation values. This state is characterized by zero or low positive correlation values. This was the most frequently visited state, as participants spent an average of 88% of the time ( $SD = 13.65$ ) in this state.

**Pre-State 2 ( $M = 11.85\%$ ,  $SD = 13.65$ )**



*Figure 6:* Pre-State 2. The color bar indicates the Pearson correlation values. This state is characterized by moderate positive correlations between left (LH) and right (RH) hemispheres of visual, somatomotor, dorsal attention, and saliency/ventral attention regions. Furthermore, zero or low negative correlations were observed between all other remaining brain regions. Participants spent less time in this state ( $M = 11.85\%$ ,  $SD = 13.65$ ).

## Standard Deviation of Pre-State 1 and 2

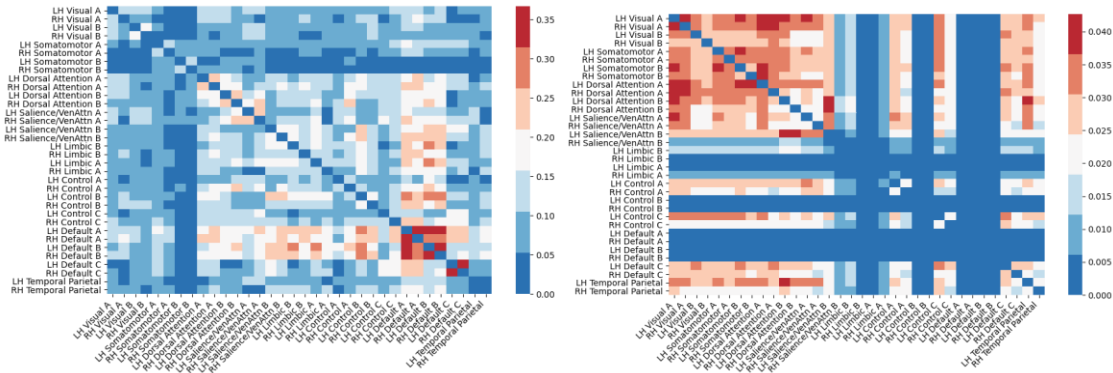


Figure 7: Standard deviation of pre-State 1 and 2 on the left and right, respectively. The average standard deviation within pre-State 1 (mean standard deviation = 0.11) is higher than pre-State 2 (mean standard deviation = 0.01).

### State Change Results: Pre-Resting-State fMRI

The number of state changes in the pre-task rsfMRI data (pre-state change) was compared between the High and Low M-capacity groups. The results showed that there was no significant difference between the number of state changes between the High ( $M = 3.30$ ,  $SD = 3.49$ ,  $n = 10$ ) and the Low ( $M = 4.1$ ,  $SD = 3.98$ ,  $n = 9$ ) M-capacity groups in the average number of state changes,  $t(17) = 0.44$   $p = 0.66$ . Figure 8 below provides a bar plot of the results.

### Average Pre-State Change for High and Low M-Capacity Groups

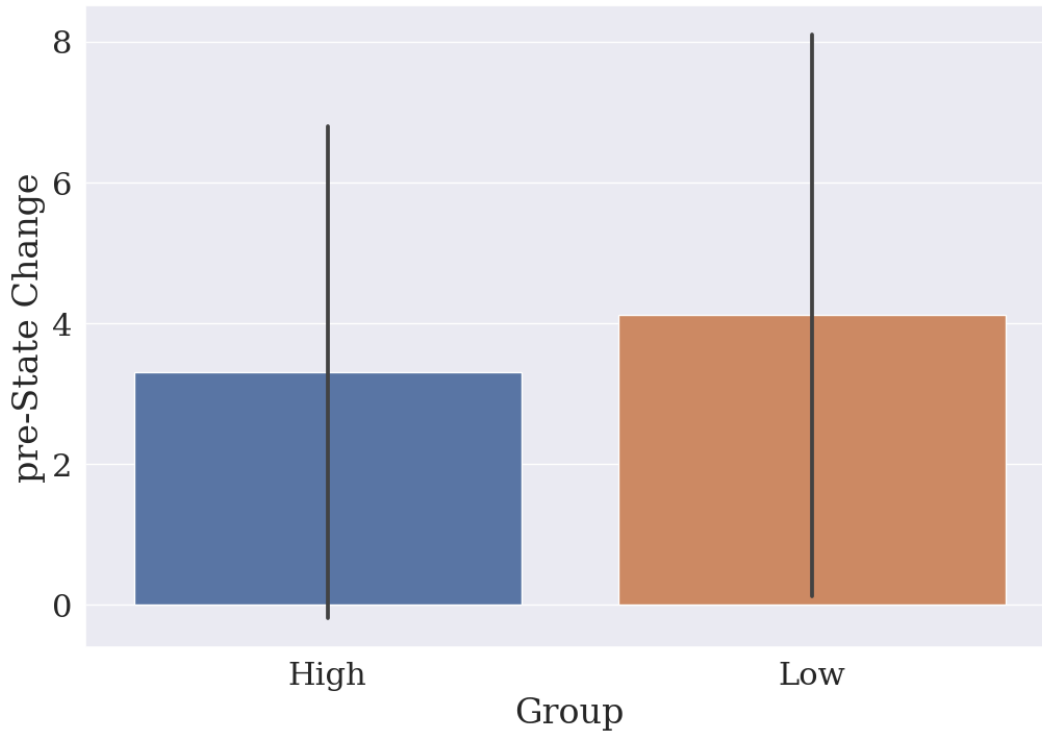


Figure 8: Bar plot of the state change for the High ( $M = 3.30$ ,  $SD = 3.49$ ,  $n = 10$ ) and the Low ( $M = 4.1$ ,  $SD = 3.98$ ,  $n = 9$ ) M-capacity groups when dFC analysis was conducted on their combined data. There was no significant difference between the two groups.

Kendall's Tau correlation was calculated to further investigate the relationship between state change and M-capacity scores. The choice of Kendall's Tau was due to the data not being normally distributed and the presence of identical M-capacity scores in the data. The results indicated that there was no significant relationship between number of state changes and M-capacity scores ( $n = 19$ ),  $r_t = -0.13$ ,  $p = 0.48$  across the entire group. Figure 9 below shows a plot of the ranked correlation (bootstrapped confidence intervals are shown as the shaded area around the line of best fit).

### Ranked Correlation Between M-Capacity and Pre-State Change

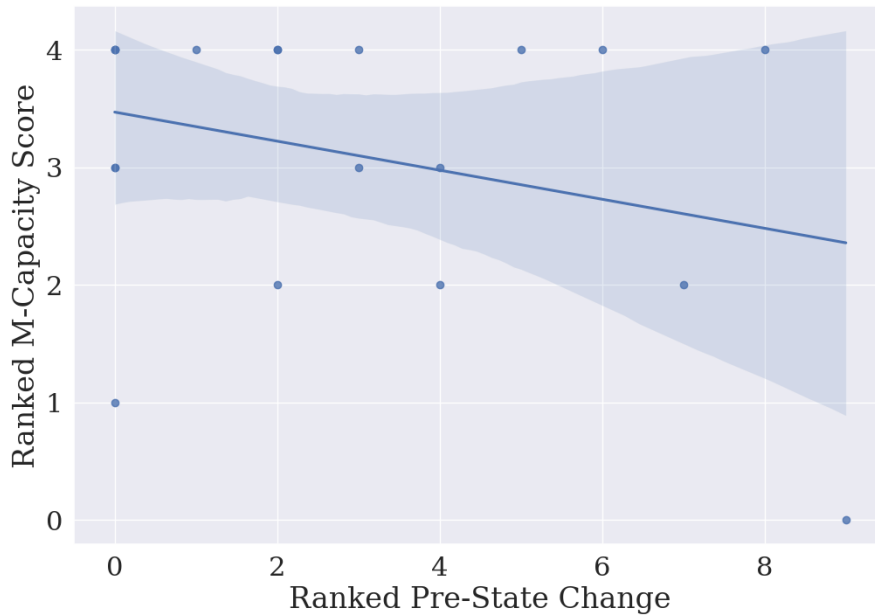


Figure 9: Ranked correlation between M-Capacity scores and pre-state change ( $n = 19$ ). There was no significant relationship between the two.

Alternatively, it is possible that the High M-capacity group had a different dFC structure compared to the Low M-capacity group. Therefore, any differences between the two groups may have been eliminated by combining their data. Therefore, dFC analysis was conducted on the High and Low M-capacity groups separately and their state change values were compared. The states obtained from this analysis are illustrated in Appendix B. The results indicated that the number of state changes for the High ( $M = 2.70$ ,  $SD = 2.41$ ,  $n = 10$ ) and the Low ( $M = 3.77$ ,  $SD = 3.18$ ,  $n = 9$ ) M-capacity groups was not significantly different,  $t(17) = 0.79$ ,  $p = 0.44$ . Figure 10 shows the plot of state change for the High and Low M-capacity groups when dFC was conducted on their data separately.

### Average Pre-State Change for High and Low M-capacity groups (Separate Analysis)

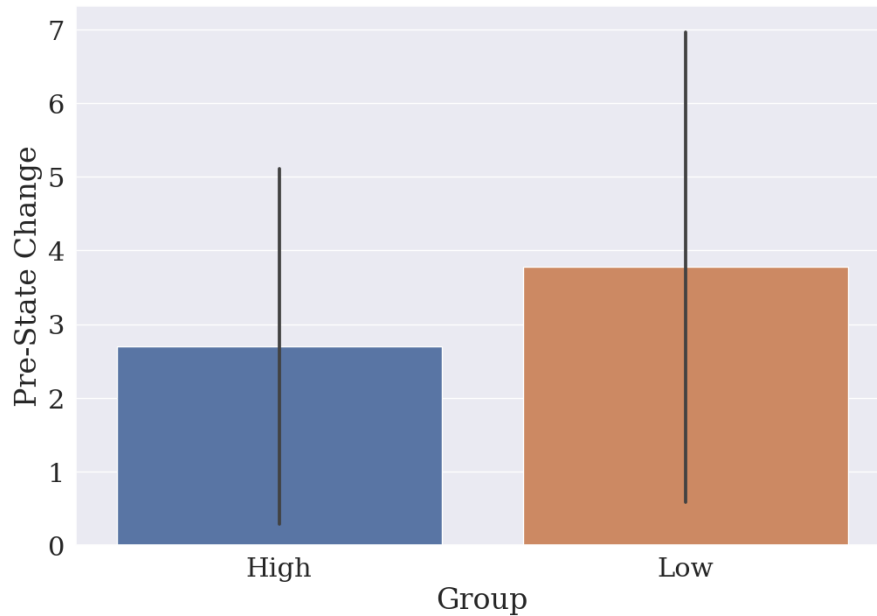


Figure 10: The number of state changes computed from applying dFC analysis to the High ( $M = 2.70$ ,  $SD = 2.41$ ,  $n = 10$ ) and Low ( $M = 3.77$ ,  $SD = 3.18$ ,  $n = 9$ ) M-capacity groups separately. There was no significant difference between the two groups.

Since there was a ceiling effect in the M-capacity scores, a Kendall's Tau correlation was conducted to investigate the relationship between state change and M-capacity in the Low M-capacity group. There was no significant correlation ( $n = 9$ ),  $r_{\tau} = -0.27$ ,  $p = 0.35$ . Figure 11 shows the ranked correlation between M-capacity scores and pre-state change for the Low M-capacity group.



## Ranked Correlation Between Low M-Capacity Group's Scores and Pre-State Change

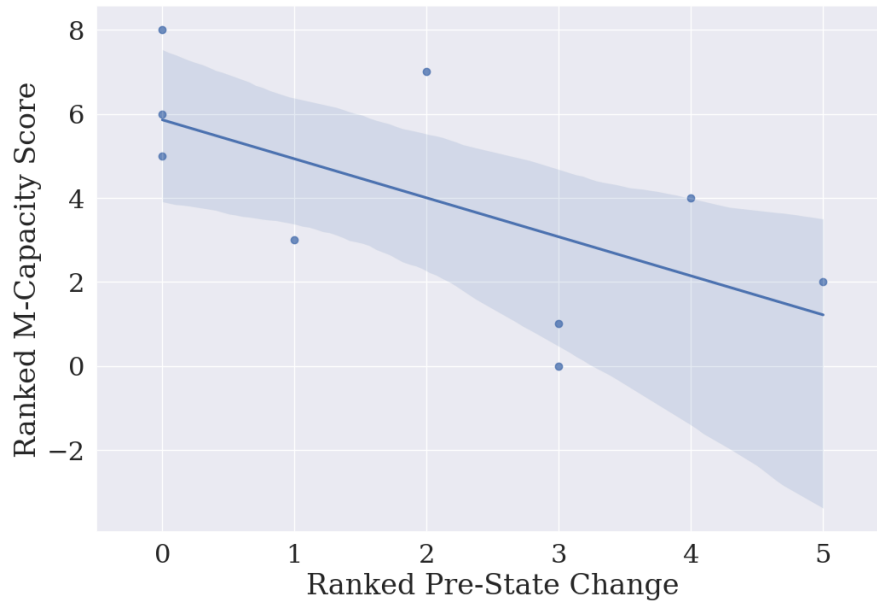


Figure 11: Ranked correlation between M-capacity scores and pre-state change when dFC was applied separately to the Low M-capacity group ( $n = 9$ ). The correlation was not found to be significant.

### *Dwell Time Results: Pre-Resting-State fMRI*

The average dwell time for each participant was obtained after conducting dFC on all participants. The average dwell time in State 1 for the High ( $M = 38.25$ ,  $SD = 57.98$ ,  $n = 10$ ) and Low ( $M = 17.52$ ,  $SD = 17.41$ ,  $n = 9$ ) M-capacity groups was not significantly different,  $t(17) = 0.97$ ,  $p = 0.34$ . The average dwell time in State 2 for the High ( $M = 2.71$ ,  $SD = 3.31$ ,  $n = 10$ ) and Low ( $M = 2.35$ ,  $SD = 3.24$ ,  $n = 9$ ) M-capacity groups was also not significantly different,  $t(17) = 0.22$ ,  $p = 0.82$ . Figure 12 illustrates the average dwell time for States 1 and 2 of the High vs Low M-capacity groups.

### Average Dwell Time in States 1 and 2 for High and Low M-capacity Groups

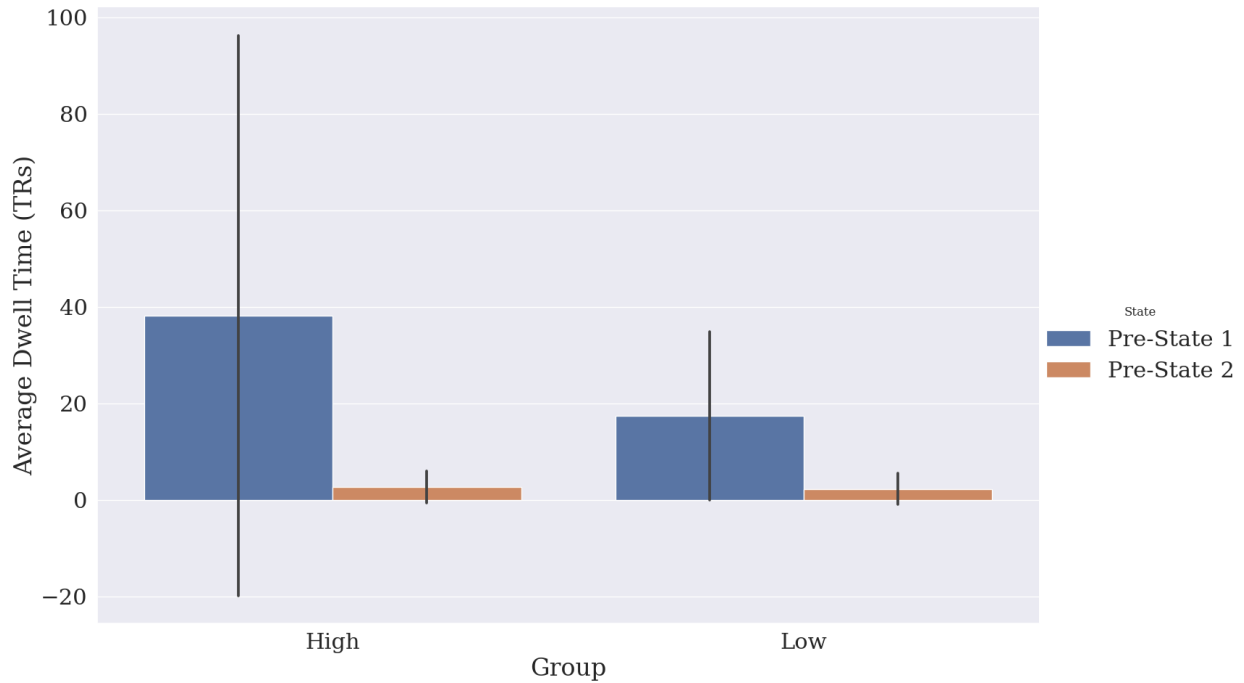


Figure 12: Average dwell time (TRs) in States 1 and 2 for High and Low M-capacity groups. The y-axis displays dwell time in number of TRs. No significant difference was found between average dwell time in the High and Low M-capacity groups in pre-States 1 or 2.

Kendalls Tau correlation was calculated to determine the relationship between M-capacity scores and dwell time in pre-States 1 and 2. The correlation between M-capacity and the average dwell time in pre-State 1 ( $n = 19$ ) approached significance (did not survive Bonferroni correction for multiple comparisons),  $r_{\tau} = 0.35, p = 0.05$ . There was no correlation between M-capacity and average dwell time in pre-State 2,  $r_{\tau} = -0.01, p = 0.93$ . Figures 13 and 14 show the Kendall's Tau correlation between M-capacity scores and average dwell time for pre-States 1 and 2, respectively.

### Ranked Correlation Between M-Capacity Scores and Average Dwell Time in State 1

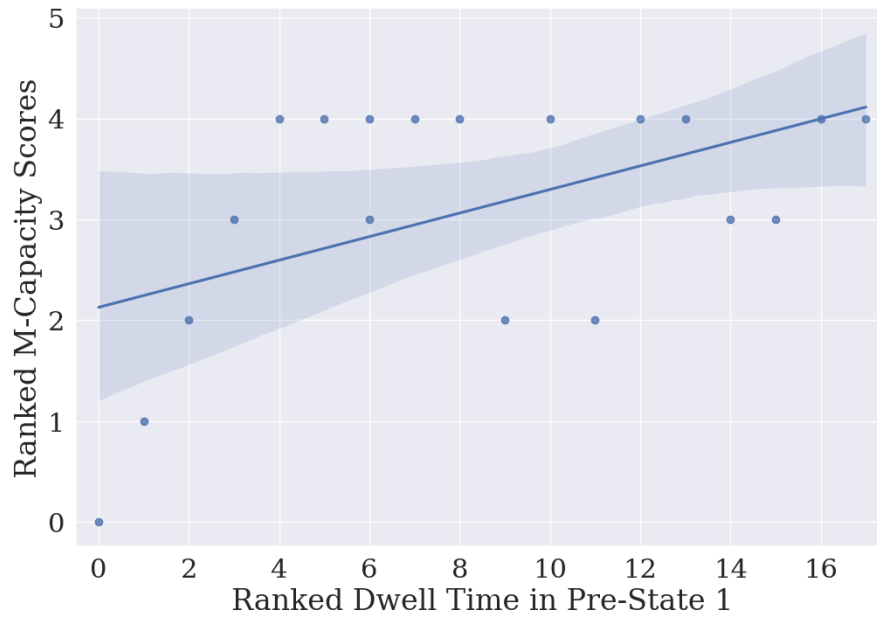


Figure 13: Ranked correlation between M-capacity scores and average dwell time in State 1 ( $n = 19$ ). The correlation approached significance (did not survive Bonferroni correction for multiple comparisons).

## Ranked Correlation Between M-Capacity Scores and Average Dwell Time in State 2

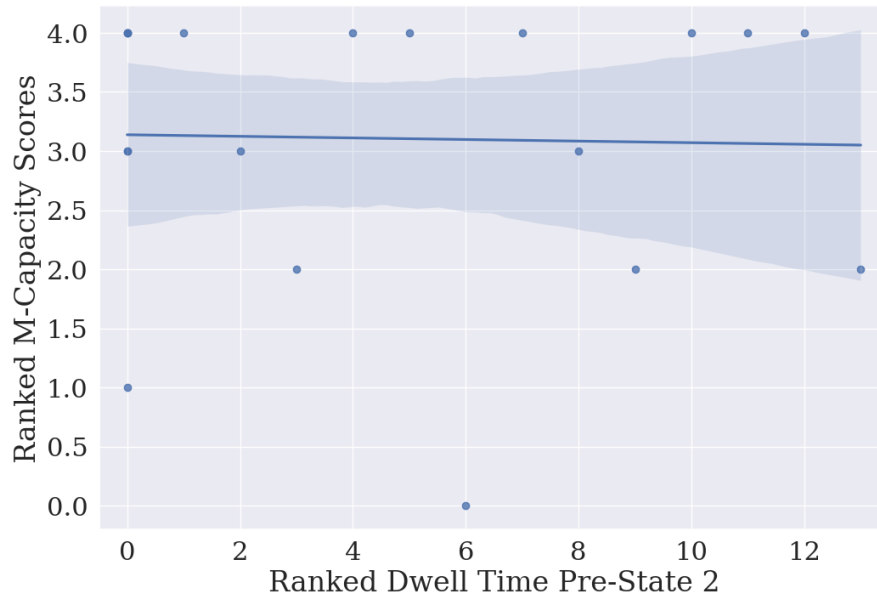


Figure 14: Ranked correlation between M-capacity scores and the average dwell time in State 2 ( $n = 19$ ). The correlation was not significant.

Similarly, to take into consideration that the High and Low M-capacity groups may have had different dFC structures, this analysis was done on the groups separately. Then, the average dwell time for the two groups was compared. The average dwell in State 1 for the High ( $M = 71.57$ ,  $SD = 67.54$ ,  $n = 10$ ) and Low ( $M = 33.68$ ,  $SD = 35.31$ ,  $n = 9$ ) M-capacity groups was not significantly different,  $t(17) = 1.42$ ,  $p = 0.17$ . The average dwell time in State 2 for the High ( $M = 3.96$ ,  $SD = 4.39$ ,  $n = 10$ ) and Low ( $M = 4.18$ ,  $SD = 4.90$ ,  $n = 9$ ) M-capacity groups was also not significantly different,  $t(17) = -0.09$ ,  $p = 0.92$ . The results are shown in Figure 15 for both states.

### Average Dwell Time of High and Low M-capacity Groups in States 1 and 2

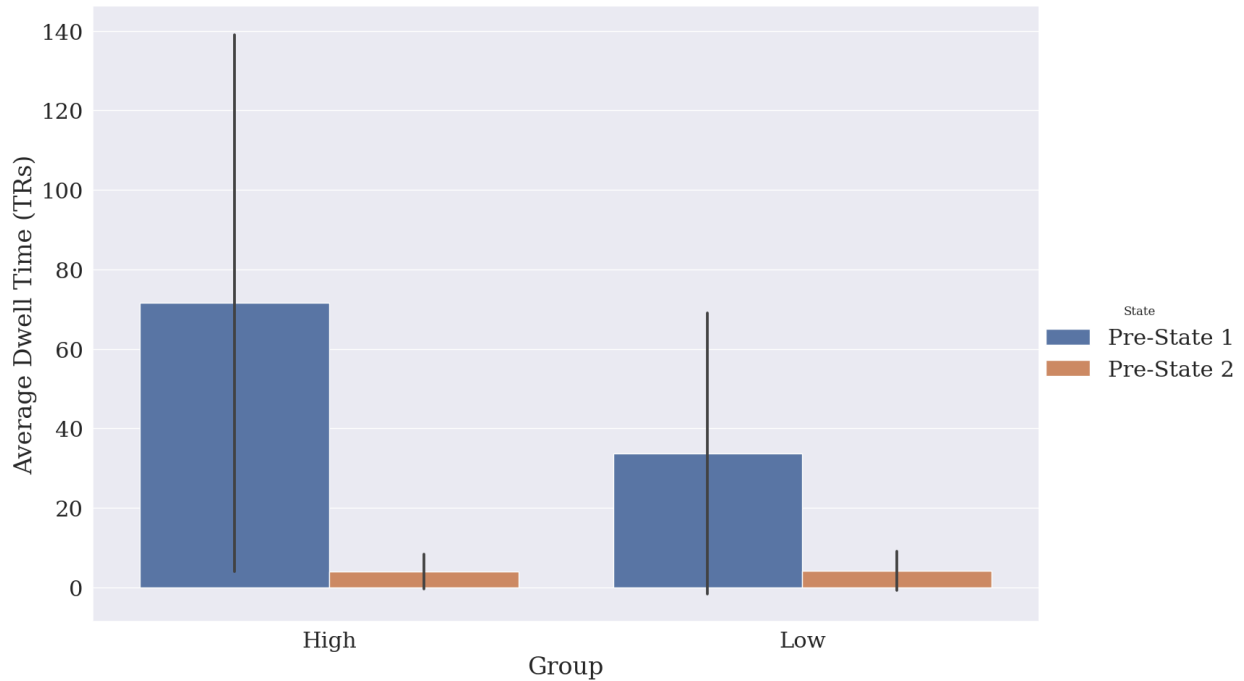


Figure 15: Average dwell time (TRs) of High and Low M-capacity groups when dFC was applied to the groups separately. There was no significant difference between the respective states between the groups.

Kendall's Tau correlation was conducted to investigate the relationship between M-capacity and average dwell time in pre-States 1 and 2 in the Low M-capacity group ( $n = 9$ ) only. There was a significant positive Kendall's Tau correlation between average dwell time in pre-State 1 and M-capacity scores in the Low M-capacity group (corrected for multiple comparisons),  $r_{\tau} = 0.80$ ,  $p < 0.01$ . However, the Kendall's Tau correlation of average dwell time in pre-State 2 and M-capacity scores in the Low M-capacity group was not significant,  $r_{\tau} = -0.16$ ,  $p = 0.56$ . Figures 16 and 17 show the plot of ranked correlation between the Low group's M-capacity scores and average dwell time in pre-States 1 and 2, respectively.

## Ranked Correlation Between Low Group's M-Capacity Scores and Average Dwell Time in State 1

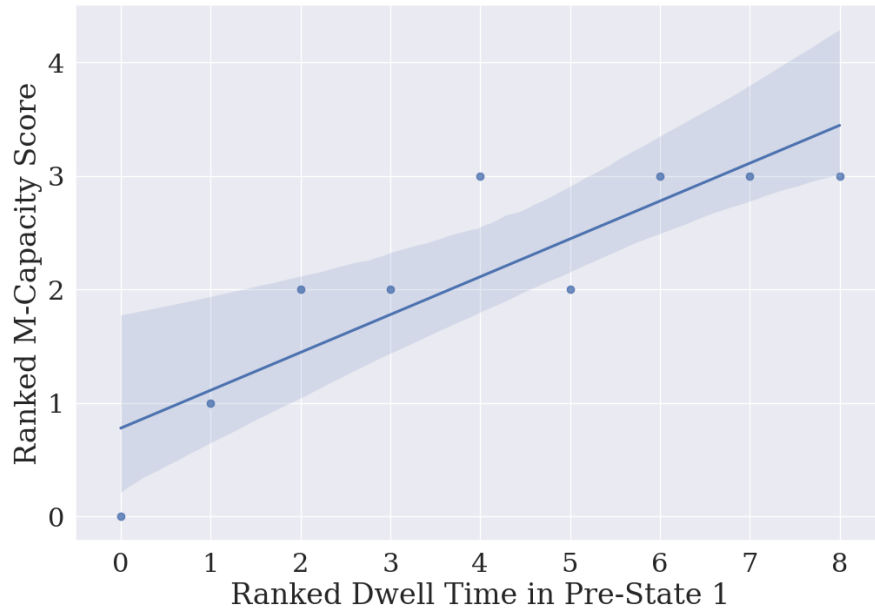


Figure 16: Ranked correlation between M-capacity scores of the Low group and average dwell time in State 1 when dFC was applied to the groups separately. There was a significant positive correlation ( $n = 9$ ). Higher average dwell time in pre-State 1 was related to higher M-capacity scores.

## Ranked Correlation Between Low Group's M-Capacity Scores and Average Dwell Time in State 2

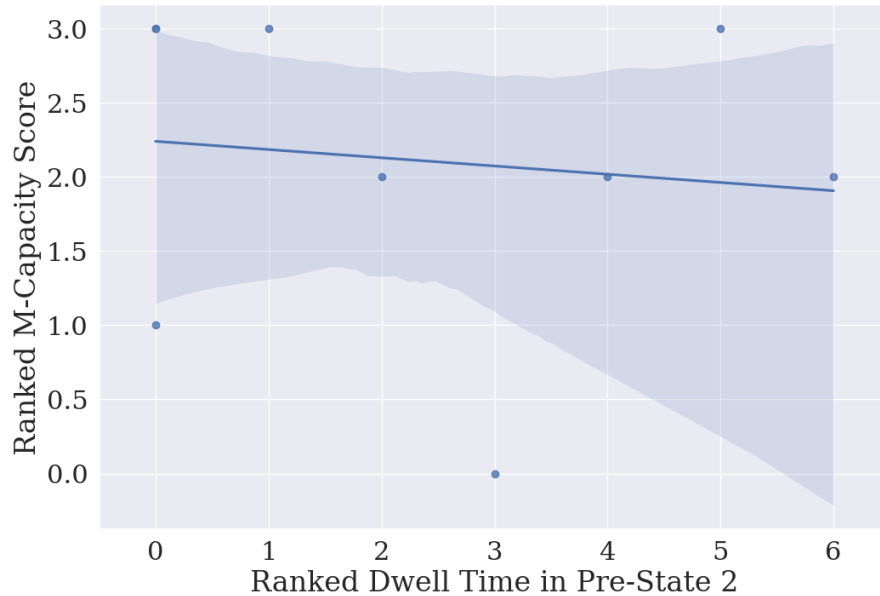


Figure 17: Ranked correlation between M-capacity score of the Low group and dwell time in State 2 when dFC was applied to the groups separately ( $n = 9$ ). The correlation was not significant.

### Comparison of States Between the High and Low M-Capacity Groups

DFC analysis was separately applied to the High ( $n = 10$ ) and Low ( $n = 9$ ) M-capacity groups in the previous step. The difference between the pre-States 1 and 2 for the two M-capacity groups was computed and tested for significance and controlled for multiple comparisons using the Bonferroni method. Figures 18 and 19 show the p-values (upper right half) and the difference between the Pearson correlation values (lower left half) comparing the two groups in pre-States 1 and 2. The color bar on the left indicates the Pearson correlation values and the one on the right indicates the p-values. No significant group difference was found for any pairwise correlations of the nodes within either state.

## Correlation Difference and P-Values of State 1 Between High and Low M-Capacity Groups

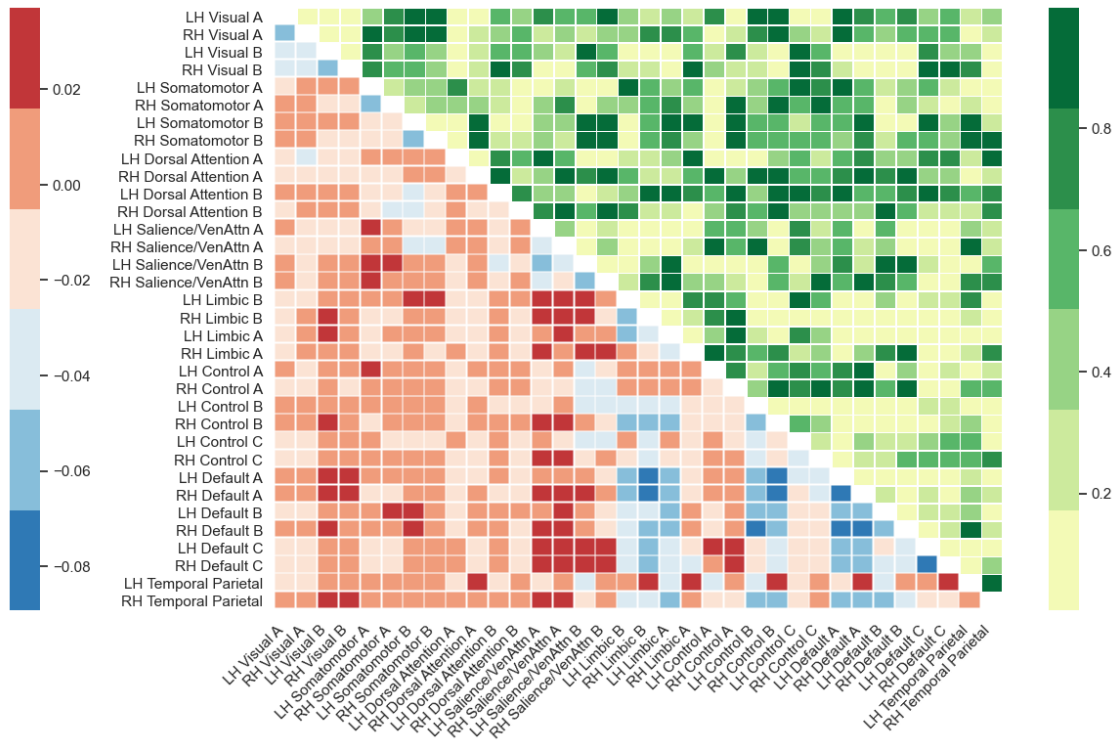


Figure 18: Difference in Pearson correlation values (lower left half) and p-value (upper right half) between State 1 of the High ( $n = 10$ ) and Low ( $n = 9$ ) M-capacity groups. The color bar on the left indicates Pearson correlation and the one on the right indicates p-values. No significant difference was found.



## Correlation Difference and P-Values of State 2 Between High and Low M-Capacity Groups

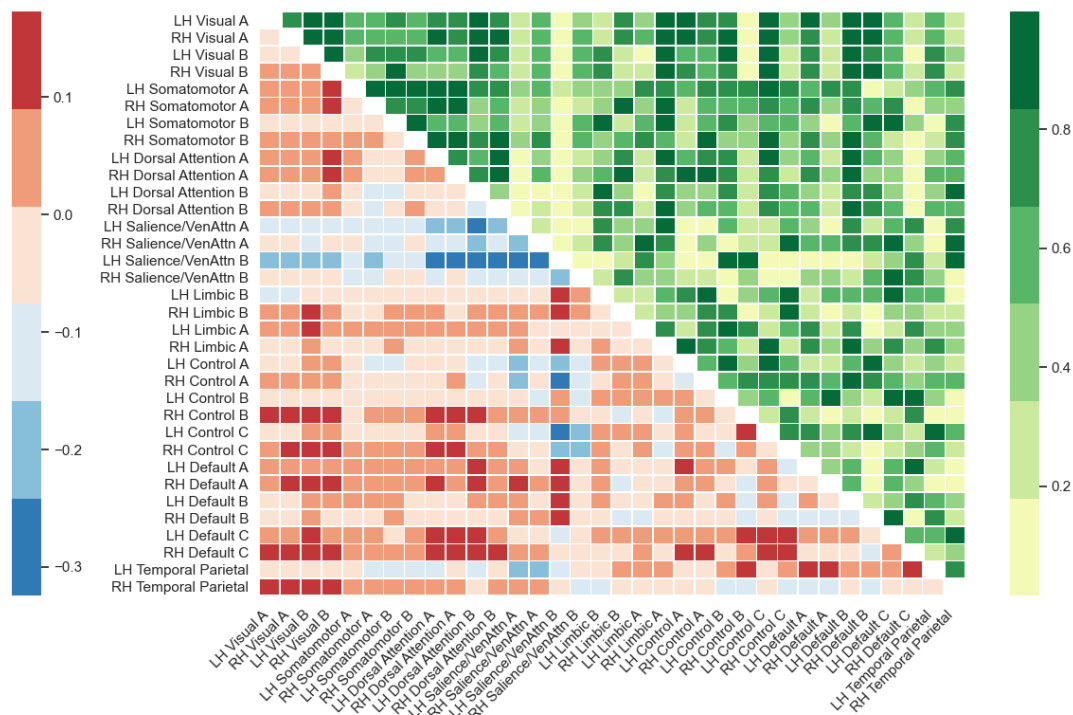


Figure 19: Difference in Pearson correlation values (lower left half) and p-value (upper right half) between State 2 of the High ( $n = 10$ ) and Low ( $n = 9$ ) M-capacity groups. The color bar on the left indicates the Pearson correlation values and the one on the right indicates the p-values. No significant difference was found.

## Results Related to Testing of the Second Hypothesis

### State Change and Dwell Time Between the Pre- and Post-Resting-State fMRI

To test whether engagement in the task measuring M-capacity transiently altered dFC parameters, the participants' state change and dwell time before and after the task were compared. Out of the 19 participants who had a pre-task rsfMRI data, only 8 completed a post-task rsfMRI session. Therefore, only 8 participants' data who had both pre- and post-task rsfMRI scans were included in this analysis. The state change for the pre- ( $M = 3.625$ ,  $SD = 3.03$ ,  $n = 8$ ) and post-task rsfMRI ( $M = 2.75$ ,  $SD = 2.81$ ,  $n = 8$ ) was not significantly different,  $t(7) = 1.07$ ,  $p$

= 0.31. Figure 20 shows the average state change of the pre- and post-task rsfMRI data. The average dwell time in State 1 for the pre- ( $M = 28.42$ ,  $SD = 26.72$ ,  $n = 8$ ) and post-task rsfMRI ( $M = 31.12$ ,  $SD = 23.04$ ,  $n = 8$ ) was also not significantly different,  $t(7) = -1.46$ ,  $p = 0.18$ . The average dwell time in State 2 for the pre- ( $M = 4.09$ ,  $SD = 6.24$ ,  $n = 8$ ) and post-task rsfMRI ( $M = 3.82$ ,  $SD = 4.66$ ,  $n = 8$ ) was also not found to be significantly different,  $t(7) = 0.15$ ,  $p = 0.87$ . Figure 21 shows the average dwell time in pre- and post-task rsfMRI for States 1 and 2.

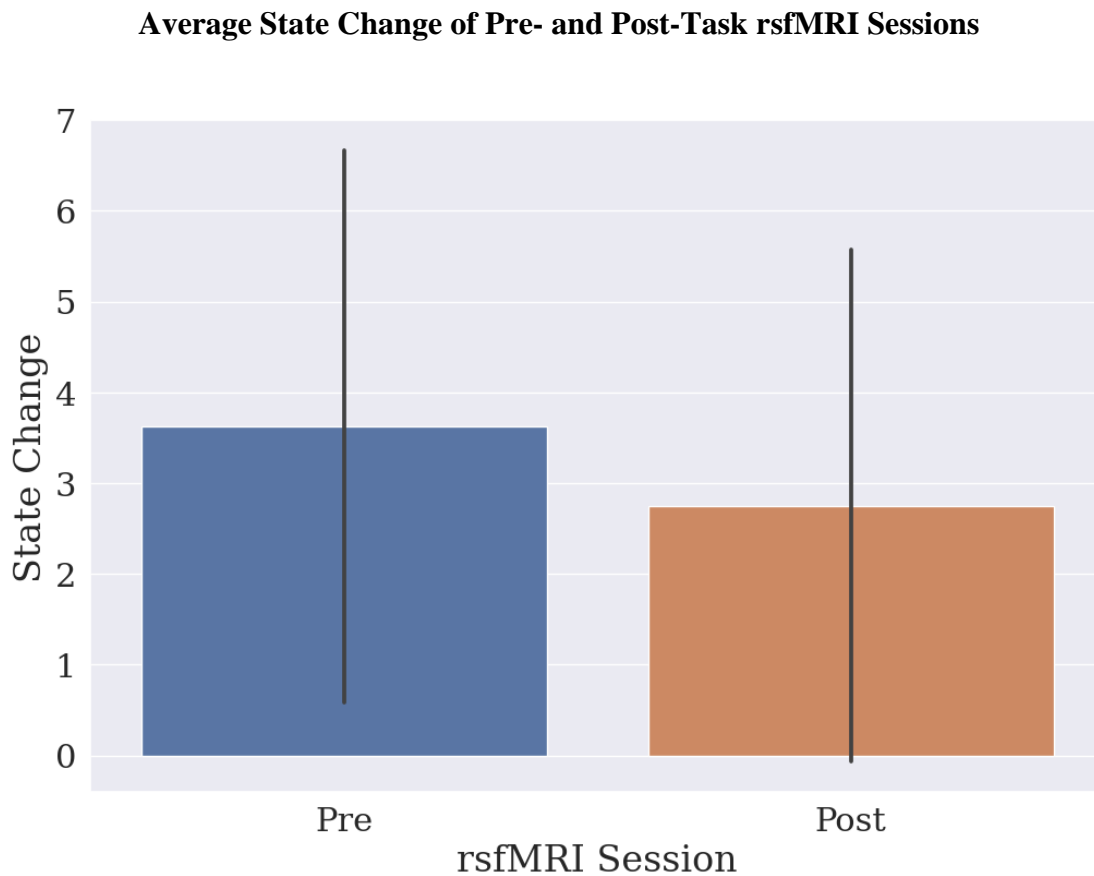


Figure 20: Mean state change of the pre- and post-task rsfMRI sessions. The difference between the pre- ( $M = 3.22$ ,  $SD = 3.08$ ,  $n = 8$ ) and post-task rsfMRI ( $M = 5.33$ ,  $SD = 4.96$ ,  $n = 8$ ) sessions was not significant.

## Average Dwell Time of High and Low M-Capacity Groups in Pre- and Post-States 1 and 2

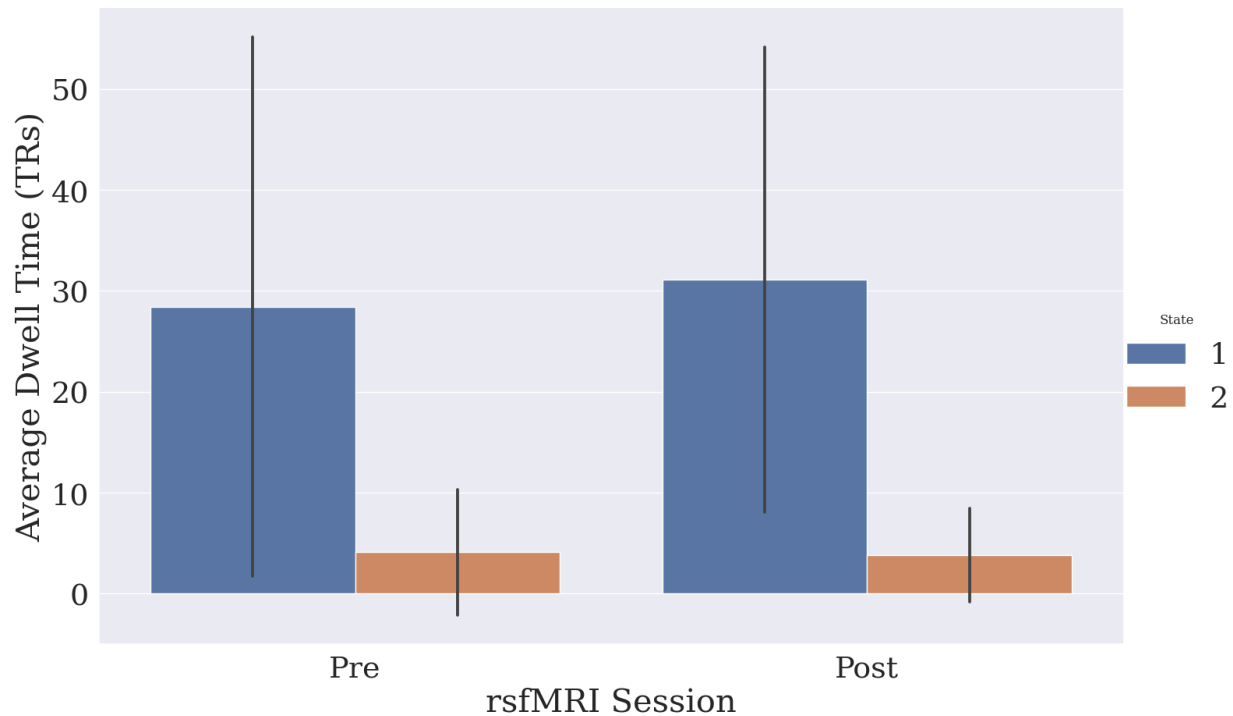


Figure 21: Average dwell time (TRs) of both State 1 and 2 of pre- and post-task rsfMRI sessions. The average dwell time of State 1 was not significantly different between the pre- ( $M = 28.42$ ,  $SD = 26.72$ ,  $n = 8$ ) and post-task rsfMRI ( $M = 4.09$ ,  $SD = 6.24$ ,  $n = 8$ ) sessions. The difference was also not significant between the pre- ( $M = 31.12$ ,  $SD = 23.04$ ,  $n = 8$ ) and post-task rsfMRI ( $M = 3.82$ ,  $SD = 4.66$ ,  $n = 8$ ) sessions of State 2.

### Comparison of Pre- and Post-States

To determine if State 1 was altered due to the M-capacity task, pre- and post-State 1 were compared. The results showed that no correlations significantly changed due to engaging in the M-capacity task. The same comparison was done with pre- and post-State 2. Figures 22 and 23 show the p-values (upper right half) and the difference between the Pearson correlation values (lower left half) comparing pre- and post-State 1 as well as pre- and post-State 2. Appendix C shows the cluster centres for post-States 1 and 2. The color bar on the left shows the Pearson

correlation values and the one on the right shows the p-values. Similarly, no region showed significantly altered correlation.

### Correlation Difference and P-Values Between Pre- and Post-State 1

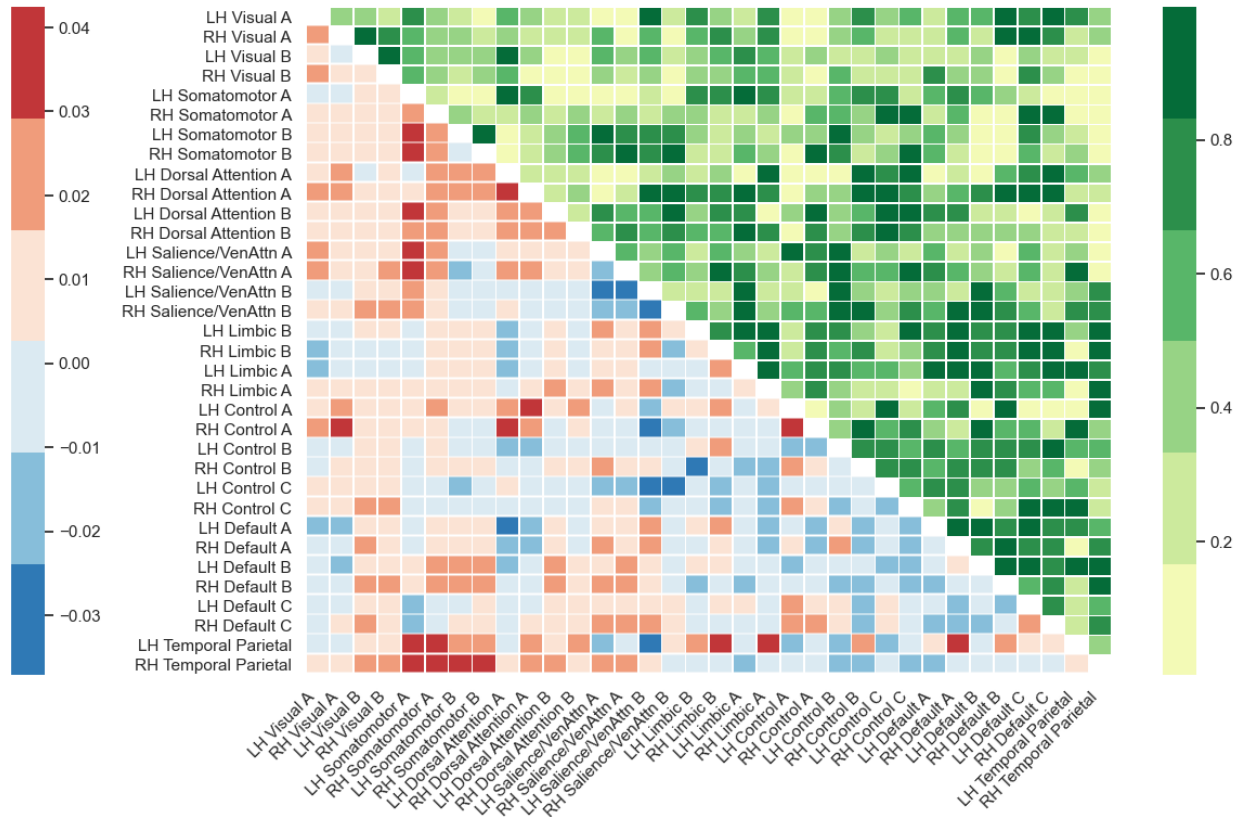


Figure 22: Difference in Pearson correlation values (lower left corner) and the p-values (upper right corner) comparing pre- and post-State 1. The color bar on the left indicates Pearson correlation and the one on the right indicates p-values. The comparison indicates that no brain region showed altered activity in this state.

## Correlation Difference and P-Values Between Pre- and Post-State 2

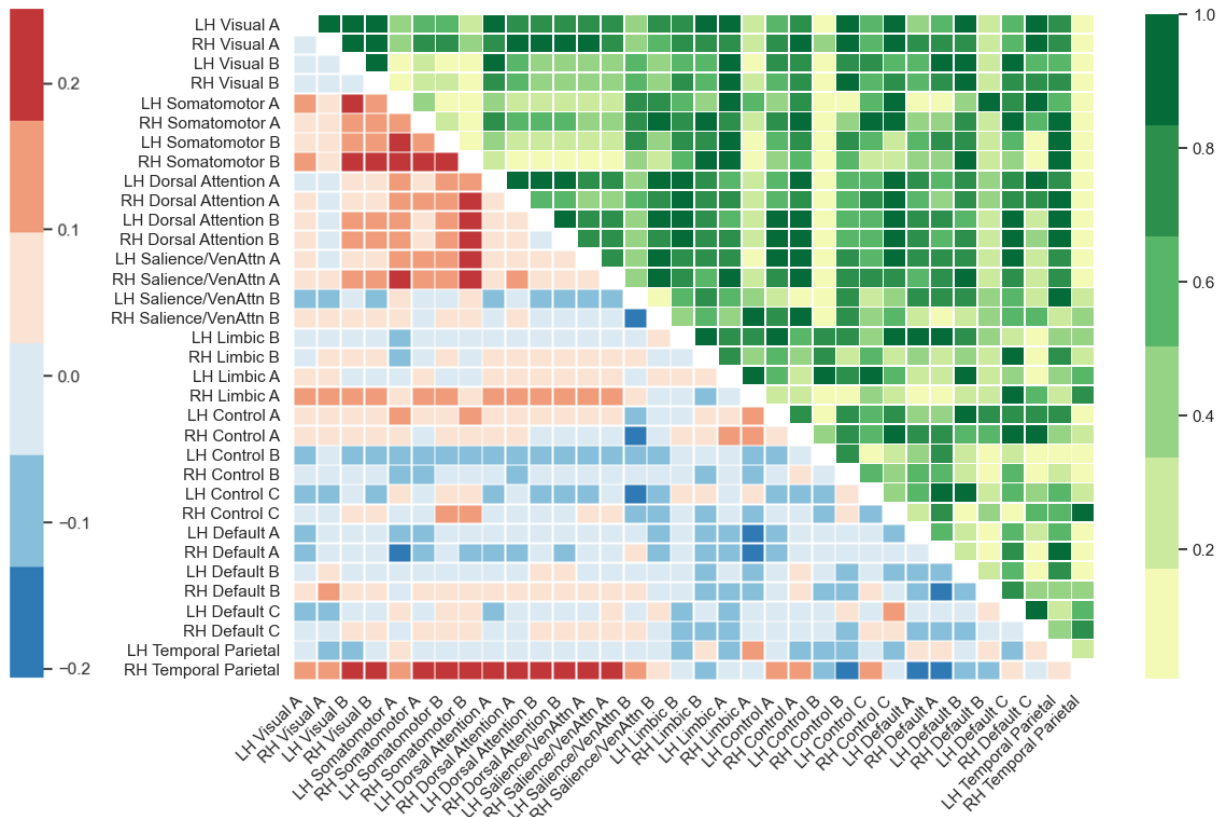


Figure 23: Difference in Pearson correlation values (lower left corner) and the p-values (upper right corner) comparing pre- and post-State 2. The color bar on the left indicates Pearson correlation and the one on the right indicates p-values. The comparison indicates that no brain region showed altered activity in this state.

## Results Related to Testing of the Third Hypothesis

The same 19 participants' fMRI data included in the original analysis with GPIP were used to conduct dFC with GIFT. The optimal number of states was also found to be two. The states are shown in below in Figure 24. The state on the left in Figure 24 occurs more frequently (72%) compared to the state on the right (28%). This state is characterized by zero or low correlation values. The state on the right which occurs less frequently is characterized by higher correlation values.

## States Obtained From Dynamic Functional Connectivity Analysis Using GIFT

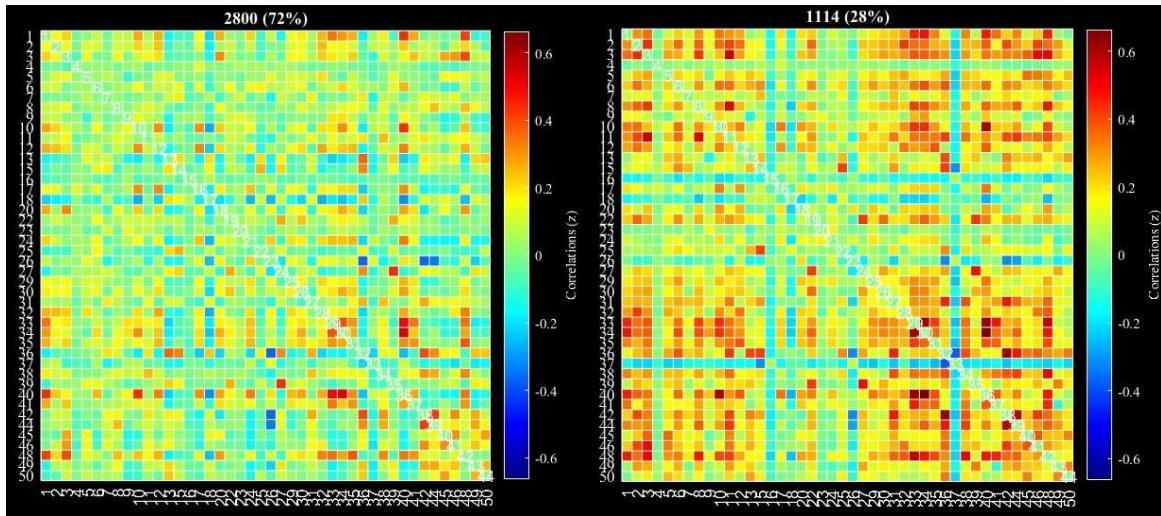


Figure 24: Two states obtained using GIFT to conduct dFC analysis on the pre-task rsfMRI data.. The state on the left occurs more frequently (72%) compared to the state on the right (28%). The state on the left is characterized by low or near zero correlation values whereas the state on the right has higher correlation values.

Furthermore, the state change for the 19 participants in the analysis conducted with GIFT ( $M = 3.16$ ,  $SD = 2.68$ ) was found to be similar to using GPIIP ( $M = 3.16$ ,  $SD = 3.68$ ) to conduct dFC analysis.

### Supplemental Analyses

#### *Correlation of M-Capacity With State Change and Dwell Time of Post-Resting-State fMRI*

Measures of state change and dwell time from the post-task rsfMRI session were correlated with M-capacity scores to further investigate any brain-behavior relationships. The Kendall's Tau correlation between state change in post-task rsfMRI and M-capacity ( $n = 8$ ) was not significant,  $r_{\tau} = -0.17$ ,  $p = 0.59$ . Figure 25 graphs the ranked correlation between post-task rsfMRI state change and M-capacity. Furthermore, the Kendall's Tau correlation between M-capacity and dwell time in post-State 1 was also not significant,  $r_{\tau} = 0.20$ ,  $p = 0.51$ . Figure 26

shows this correlation. Similarly, the Kendall's Tau correlation between dwell time in post-State 2 and M-capacity was not significant,  $r_{\tau} = -0.20$ ,  $p = 0.50$ . Figure 27 illustrates the plot of this correlation.

### Ranked Correlation Between M-Capacity Scores and State Change

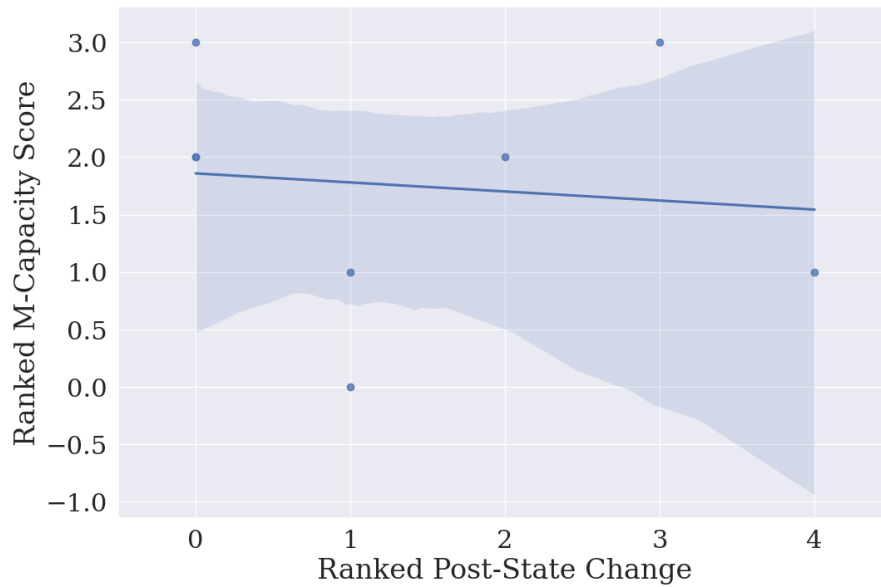


Figure 25: Ranked correlation between M-capacity and state change ( $n = 8$ ). The correlation was not significant.

### Ranked Correlation Between M-Capacity Scores and Dwell Time in State 1

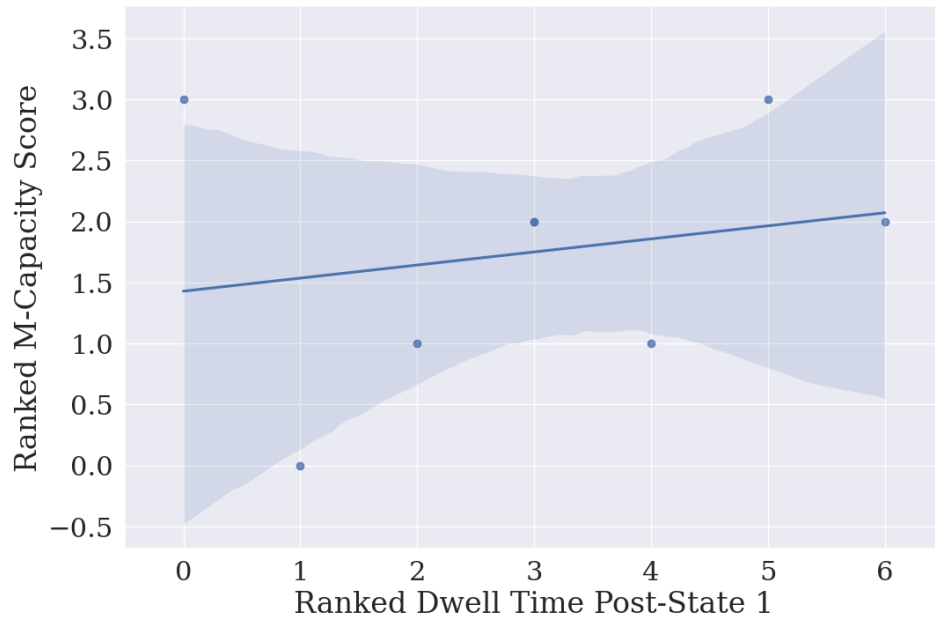


Figure 26: Ranked correlation between M-capacity and average dwell time in State 1 ( $n = 8$ ). This correlation was not significant.



### Ranked Correlation Between M-Capacity Scores and Dwell Time in State 2

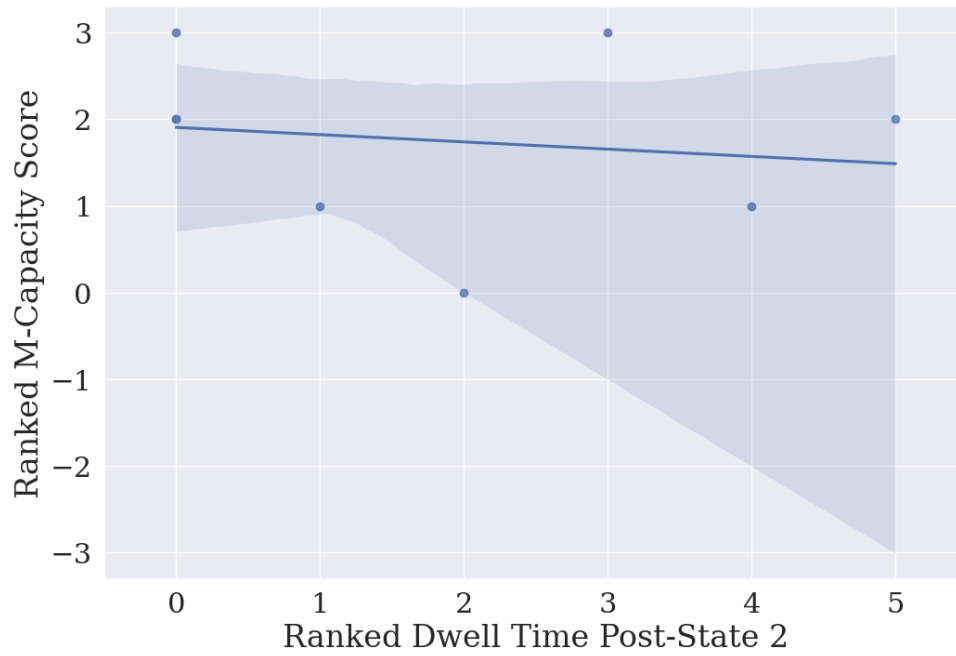


Figure 27: Ranked correlation between M-capacity scores and average dwell time in State 2 ( $n = 8$ ). This correlation was not significant.

## Discussion

### Neural Flexibility and M-Capacity

The relationship between the neural dynamics of FC and M-capacity had not been previously investigated. This was explicitly tested by comparing measures of dFC, namely state change and dwell time, between those in the High and Low M-capacity groups from the pre-task rsfMRI session. The results showed that there were no significant differences between the two groups in any of the dFC measures. However, the correlation between dwell time in pre-State 1 and M-capacity when all the pre-task rsfMRI data were combined approached significance. Due to the ceiling effect in M-capacity scores, a separate analysis was conducted where the M-capacity scores of the Low group only were correlated with the dwell time in pre-State 1. The results were significant. This indicates that perhaps a positive correlation between dwell time in pre-State 1 and M-capacity does exist. However, the relationship is diminished by the ceiling effect in the M-capacity scores. Importantly, pre-State 1 is characterized by zero or low FC configuration with high variability. This finding is in line with previous literature showing that more frequent occupation of states characterized by zero or low FC with high variability is related to individual differences in executive function (Nomi et al., 2017). This state is reported to reflect a flexible FC configuration (Nomi et al., 2017). Because this state allows for a variety of connections ranging from positive to negative correlation to form between different brain regions. Alternatively, the less frequently occurring state is constrained in its configuration and varies much less. This view also relates to a field referred to as Coordination Dynamics (Tognoli and Kelso, 2014), which proposes that the brain adaptively moves between extremes of chaotic and rigid states. Furthermore, inline with the study by Nomi et al. (2017), no relationship between pre-State 2 and M-capacity scores was found. As such, the results support the

hypothesis that higher dwell time in a state characterized by high FC flexibility is related to scores on M-capacity.

The states obtained from conducting dFC analysis on High and Low M-capacity groups separately were compared to determine whether a group difference existed in the states themselves. The results showed no significant difference between the two groups in either pre-State 1 or 2.

### **Modulation of Dynamic Functional Connectivity**

The second hypothesis proposed that compared to the pre-task rsfMRI session, measures of dFC in the post-task rsfMRI would be altered due to the mentally demanding task completed by the participants immediately beforehand. Therefore, state change and dwell time obtained from the pre- and post-task rsfMRI sessions were compared. The results showed that there was no significant difference in the number of state changes and average dwell time between the two rsfMRI sessions. Furthermore, the states themselves were compared between the two rsfMRI sessions. The results also showed that the states did not change significantly as a result of the intervening M-capacity task. A study conducted by Stevens et al. (2010) had established that FC is modulated by prior task. However, the current study was not able to establish a modulatory effect of the CMT task (Clown version) on temporal dynamics of FC. This may have been due to the choice of the task or perhaps the low number of participants did not yield sufficient statistical power to discern such an effect. Understanding what modulates and influences dFC metrics can open novel avenues for understanding cognitive processing and even clinical intervention.

## **Use of GPIIP to Conduct Dynamic Functional Connectivity Analysis**

In addition to investigating the dynamic neural correlates of M-capacity, this study is a proof of concept that dFC analysis can be conducted on fMRI data parcellated with GPIIP. The evidence for this comes from comparison of the analysis results using GPIIP with the results using GIFT, which is a validated and established software for conducting dFC analysis. Both methods showed that the optimal number of clusters was two and both found similar state change values. In addition, both methods showed that the most frequently occurring state had near zero correlation values and the least frequently occurring state had high correlation values where network structures were visible. The only observed difference was in the frequency of occurrence of the two states. The frequency of occurrence for GPIIP and GIFT were found to be 72% and 88% for pre-State 1 and 28% and 12% for pre-State 2. Despite this difference, the pattern in the frequency of occurrence was still preserved, with the state corresponding to pre-State 1 occurring more often than the state corresponding to pre-State 2. This difference is likely due to the difference in the parcellation methods since all other steps in processing were virtually identical. Overall, the qualitative comparison provides preliminary justification for the use of GPIIP for conducting dFC. More rigorous studies providing quantitative examination of the process are needed to validate the analysis. This would be highly valuable, since many studies may be interested in taking into consideration individual differences or studying the grey matter surface of the brain exclusively.

## **Supplemental Analysis of M-Capacity and Dynamic Functional Connectivity**

The relationship between M-capacity and dFC measures from the post-task rsfMRI session was explored. No significant relationship was found between state change and dwell time with M-capacity. Since no difference was previously found between the pre- and post-task

rsfMRI sessions, it would be expected to find a relationship between M-capacity and dwell time in post-State 1. The lack of such a relationship might have been due to the lower number of participants or the fact that there was a ceiling effect in the behavioral scores of the participants who participated in the post-task rsfMRI session.

### **Comparison of Results with Prior Studies Using DFC Analysis**

It is notable that both analysis methods (i.e., parcellating with GPIP and using GIFT) indicated that the optimal number of clusters is 2. However, Nomi et al. (2017) showed that the optimal number of clusters was 5 (refer to Appendix D). On the surface, this may seem alarming. But a more detailed comparison of the clusters found in the current study and the literature resolves this discrepancy. Importantly, K-means clustering is a data-driven way to group observations. Furthermore, the clustering becomes more accurate as the number of data points increases, as it allows the algorithm to better sample the space of possible states. The current study has approximately 10 minutes of rsfMRI data from 19 participants whereas the study by Nomi et al. (2017) had approximately an hour of rsfMRI data from 189 participants. It is likely that the low number of data did not allow the algorithm to group the data into finer instantiations of the states. Instead, the data points that would have constituted a separate state on their own are grouped into two stable states. To reiterate, this does not constitute a flaw in the clustering. Instead, the clustering provides a coarser grouping.

Nomi et al. (2017) reported that the frequency of occurrence of their 5 states were 40%, 20%, 16%, 13%, and 11%. The frequency of occurrence in the current study was found to be 88% and 12%. Interestingly, the most frequently occurring state in both studies has the highest standard deviation and lowest degree of FC compared to all other states. In addition, the state with the lowest frequency of occurrence in both studies has the lowest standard deviation and

highest degree of FC. It is important to note that the 3 states between the most and least frequently occurring states outline a gradient of states between the two extremes. In other words, as the frequency of occurrence decreases, the degree of FC increases, and standard deviation decreases in a gradual way while maintaining the same FC configuration. Given this FC pattern of the states in the literature and how the low number of participants may have affected the K-means clustering algorithm, it seems very likely that the 3 intermediate states found by Nomi et al. (2017) are combined into one state or redistributed between the two states in the current study.

In the study by Nomi et al. (2017), the number of state changes was reported to be approximately 80. The current study found the state change to range between 3-4. On the surface, this may seem very different. However, it is important to consider that the number of state changes increases as the scan time increases. The study by Nomi et al. (2017) collected 6 times more data from each participant compared to the current study. Furthermore, they found five states whereas the current study found two states. The presence of five states means that there are more permutations for state change compared to having two states. These are important factors that impact the dFC measures obtained from the data.

The dwell times reported by Nomi et al. (2017) range between 40 to 80 windows. The current study found that dwell times ranged between 5 to 30 windows. It is possible that due to redistribution of the five states into two resulted this difference in dwell time values. Furthermore, increased scan duration can improve estimation of dwell times. The reason is that more opportunities are given for states to demonstrate their true amount of dwell time.

Scan time influences dFC measures such as state change and dwell time. Since it is common for studies to have different scan times, it would not be possible to directly compared

the dFC measures between studies. Therefore, it would be highly beneficial to provide metrics that allow comparison between studies. For instance, reporting the value of state change divided by the total scan time instead of directly reporting the state change. Doing so would reduce the effect of scan time on the measure of state change and allow for a more valid comparison of findings between studies. This could help solidify the metrics used to conduct dFC analysis and provide a more universal frame of reference.

### **Future Directions**

The next step in understanding the dynamic neural correlates of M-capacity would be to conduct the same study on a group of adolescents or children. M-capacity is constructed to account for the stepwise growth in cognitive processing abilities. Therefore, it would be interesting to investigate how the dFC measures of M-capacity change through development. This may also help further distinguish any differences between M-capacity and other similar constructs such as working memory.

In addition, the task measuring M-capacity should be improved to account for the higher cognitive processing abilities of certain adults in the population. This would address the ceiling effect observed in the data.

### **Limitations**

Several limitations affect this study, namely, a low number of participants, relatively short resting-state scans, as well as high attrition through the preprocessing and processing of the data. Future studies should aim for a higher number of participants and longer resting-state scan duration. Furthermore, the processing pipeline with GPIP should be further refined to retain as many participants as possible. Doing so could help reduce attrition in the final dFC analysis. The

current study used a custom-made program written in Python to conduct dFC analysis. However, certain available graphical lasso packages are not suitable for fMRI data, as it has difficulty converging on a solution. Therefore, more advanced techniques such as those employed by the skggm package should be investigate.

### **Conclusion**

The current study demonstrated a relationship between M-capacity and occupying FC states characterized by higher neural flexibility. However, dFC measures were not modulated by the cognitively demanding task. Furthermore, no other dFC measure was found to be related to M-capacity. The findings were generally in line with the extant literature. Preliminary evidence was provided as a proof of concept that similar dFC results are obtained when the parcellation of fMRI data was done with GPIP. Future studies can further delineate the dynamic neural correlates of M-capacity as it increases through development. Several limitations such as a low number of participants, shorter scan duration, and processing limitations may have affected the results.



## References

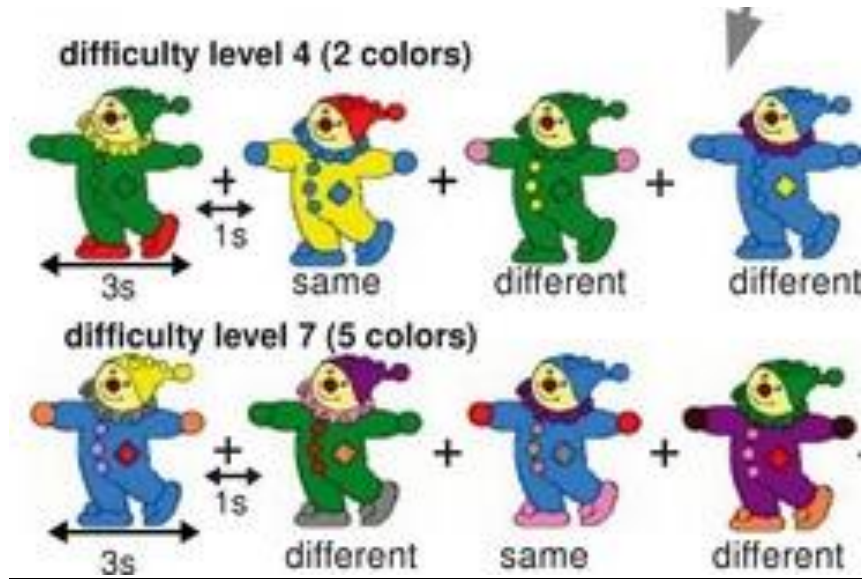
- Adelstein, J. S., Shehzad, Z., Mennes, M., DeYoung, C. G., Zuo, X. N., Kelly, C., ... & Milham, M. P. (2011). Personality is reflected in the brain's intrinsic functional architecture. *PLoS one*, 6(11), e27633.
- Allen, E. A., Damaraju, E., Plis, S. M., Erhardt, E. B., Eichele, T., & Calhoun, V. D. (2014). Tracking whole-brain connectivity dynamics in the resting-state. *Cerebral cortex*, 24(3), 663-676.
- Arsalidou, M., Pascual-Leone, J., and Johnson, J. (2010). Misleading cues improve developmental assessment of working memory capacity: the color matching tasks. *Cognitive Development*, 25(3), 262-277.
- Arsalidou, M., Pascual-Leone, J., Johnson, J., Morris, D., and Taylor, M. J. (2013). A balancing act of the brain: Activations and deactivations driven by cognitive load. *Brain and Behaviour*, 3(3), 273-285.
- Bueichekú, E., Miró-Padilla, A., & Ávila, C. (2019). Resting-state fMRI detects the effects of learning in short term: A visual search training study. *Human brain mapping*.
- Chapman, M. (1981). Pascual-Leone's theory of constructive operators. *Human Development*, 24(2), 145-155.
- Chong, M., Bhushan, C., Joshi, A. A., Choi, S., Haldar, J. P., Shattuck, D. W., ... & Leahy, R. M. (2017). Individual parcellation of resting fMRI with a group functional connectivity prior. *NeuroImage*, 156, 87-100.
- Deary, I. J. (2012). Intelligence. *Annual Review of Psychology*, 63, 453– 482.

- DuPre, E., Salo, T., Markello, R., Kundu, P., Whitaker, K., & Handwerker, D. (2019). ME-ICA/tedana: 0.0.6.
- Fischl, B. (2012). FreeSurfer. *Neuroimage*, 62(2), 774-781.
- Hillman, E. M. (2014). Coupling mechanism and significance of the BOLD signal: a status report. *Annual review of neuroscience*, 37, 161-181.
- Hutchison, R. M., & Morton, J. B. (2015). Tracking the brain's functional coupling dynamics over development. *Journal of Neuroscience*, 35(17), 6849-6859.
- Hutchison, R. M., Womelsdorf, T., Allen, E. A., Bandettini, P. A., Calhoun, V. D., Corbetta, M., ... & Handwerker, D. A. (2013). Dynamic functional connectivity: promise, issues, and interpretations. *Neuroimage*, 80, 360-378.
- Jia, H., Hu, X., & Deshpande, G. (2014). Behavioural relevance of the dynamics of the functional brain connectome. *Brain connectivity*, 4(9), 741-759.
- Kemps, E., De Rammelaere, S., and Desmet, T. (2000). The development of working memory: Exploring the complementarity of two models. *Journal of Experimental Child Psychology*, 77(2), 89-109.
- Kirchner, W. K. (1958). Age differences in short-term retention of rapidly changing information. *Journal of Experimental Psychology*, 55(4), 352-358.
- Koyama, M. S., Di Martino, A., Zuo, X. N., Kelly, C., Mennes, M., Jutagir, D. R., ... & Milham, M. P. (2011). Resting-state functional connectivity indexes reading competence in children and adults. *Journal of Neuroscience*, 31(23), 8617-8624.

- Nomi, J. S., Vij, S. G., Dajani, D. R., Steimke, R., Damaraju, E., Rachakonda, S., ... & Uddin, L. Q. (2017). Chronnectomic patterns and neural flexibility underlie executive function. *Neuroimage*, *147*, 861-871.
- Pascual-Leone, J. (1970). A mathematical model for the transition rule in Piaget's developmental stages. *Acta psychologica*, *32*, 301-345.
- Pascual-Leone, J. (2000). Reflections on working memory: Are the two models complementary?. *Journal of Experimental Child Psychology*, *77*(2), 138-154.
- Pascual-Leone, J., and Johnson, J. (2005). A dialectical constructivist view of developmental intelligence. *Handbook of understanding and measuring intelligence*, 177-201.
- Stevens, W. D., Buckner, R. L., & Schacter, D. L. (2009). Correlated low-frequency BOLD fluctuations in the resting human brain are modulated by recent experience in category-preferential visual regions. *Cerebral cortex*, *20*(8), 1997-2006.
- Stevens, W. D., & Spreng, R. N. (2014). Resting-state functional connectivity MRI reveals active processes central to cognition. *Wiley Interdisciplinary Reviews: Cognitive Science*, *5*(2), 233-245.
- Tognoli, E., & Kelso, J. S. (2014). The metastable brain. *Neuron*, *81*(1), 35-48.
- Waites, A. B., Stanislavsky, A., Abbott, D. F., & Jackson, G. D. (2005). Effect of prior cognitive state on resting-state networks measured with functional connectivity. *Human brain mapping*, *24*(1), 59-68.

Yeo, B. T., Krienen, F. M., Sepulcre, J., Sabuncu, M. R., Lashkari, D., Hollinshead, M., ... & Fischl, B. (2011). The organization of the human cerebral cortex estimated by intrinsic functional connectivity. *Journal of neurophysiology*.

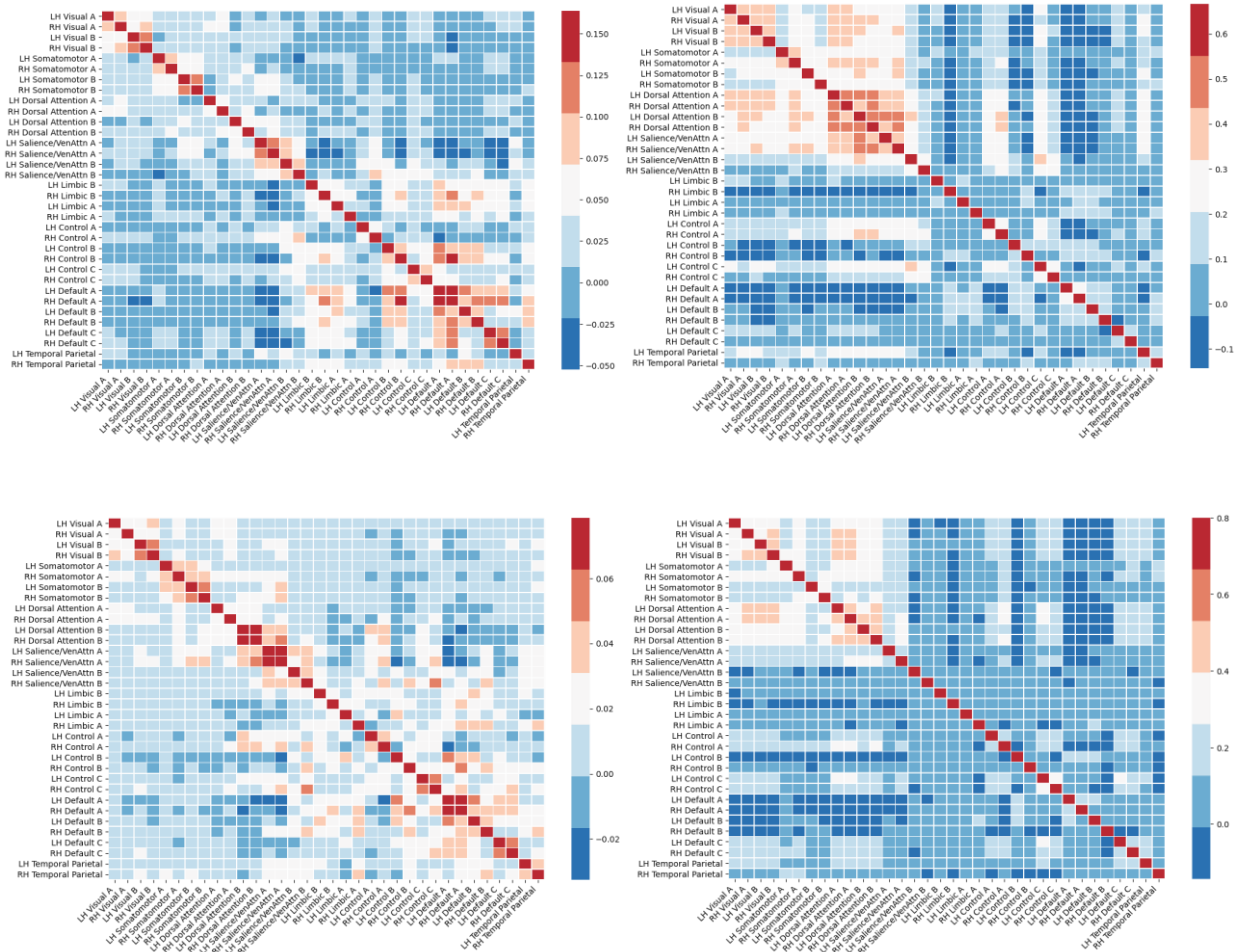
## Appendix A



### Sample Clown version of Colour Matching Task

In this version of the CMT, the participant must ignore blue and green colours as well the features of the clown's face and respond whether the stimulus they are viewing currently is the same (i.e., has the same set of colours, regardless of location) as the stimulus they were presented immediately beforehand.

## Appendix B

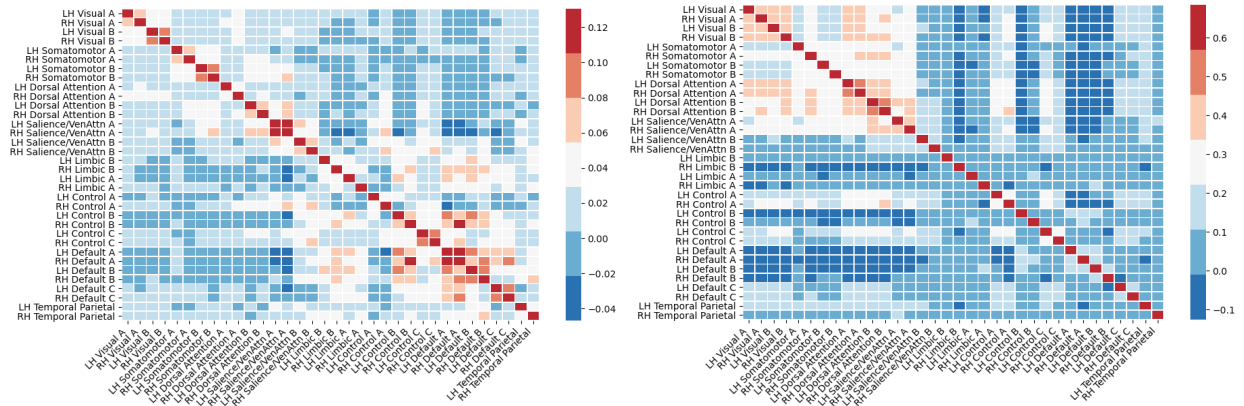


States from Conducting Dynamic Functional Connectivity on High and Low M-Capacity Groups

Separately

Shows the dFC results for pre-States 1 (left) and 2 (right) of Low group are shown in the first row when the clusters are separately computed. Similarly, the results for the High groups are shown in the second row.

## Appendix C

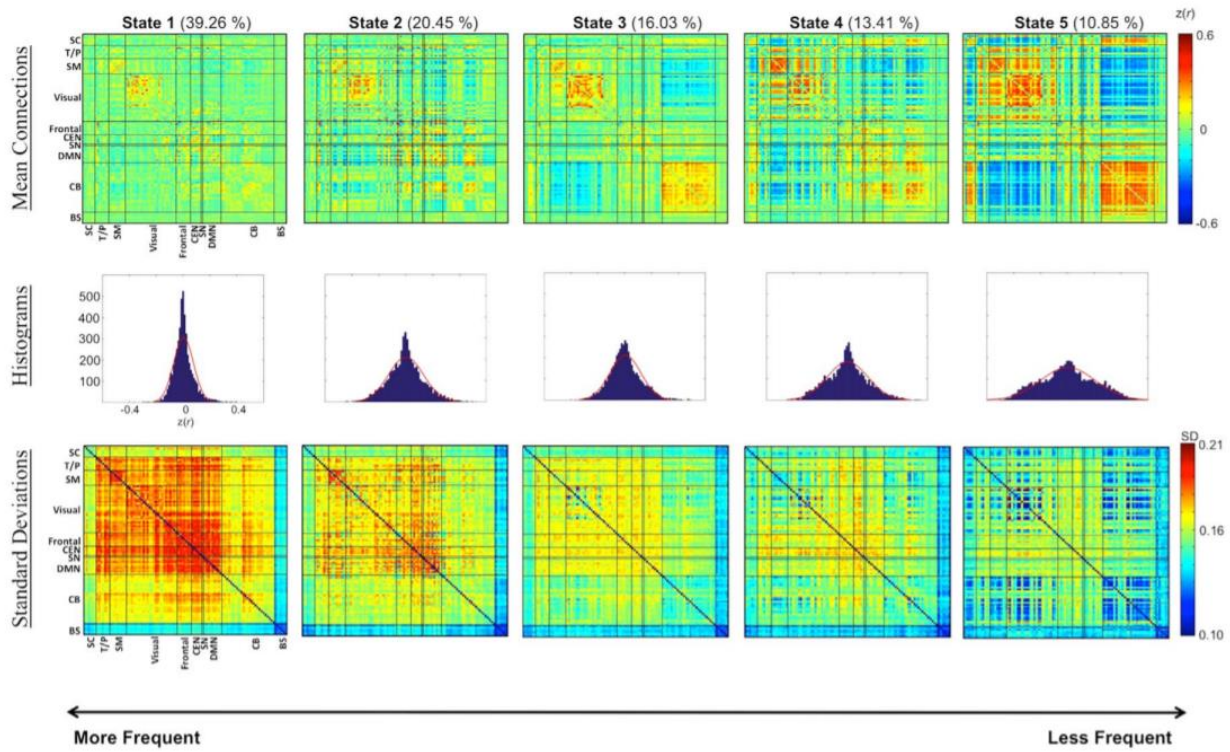


### Post-Resting-State fMRI States

Shows the cluster centers from applying dFC on the post-task rsfMRI data. Post-States 1 and 2 are shown on the left and right, respectively.

## Appendix D

### Dynamic Functional Network Connectivity – Overall Analysis



### Sample Dynamic Functional Connectivity Results From Literature

Shows the states found in the study by Nomi et al. (2017). They reported finding 5 states occurring approximately 40%, 21%, 16%, and 11% of the time. Furthermore, the more frequently occurring states have higher standard deviation compared to states occurring less frequently.